

Fine-tuning gibberellin improves rice alkali-thermal tolerance and yield

<https://doi.org/10.1038/s41586-024-08486-7>

Received: 8 November 2023

Accepted: 4 December 2024

Published online: 29 January 2025

 Check for updates

Shuang-Qin Guo^{1,2,3,6}, Ya-Xin Chen^{1,3,6}, Ya-Lin Ju^{1,3}, Chen-Yang Pan^{1,3}, Jun-Xiang Shan^{1,4}, Wang-Wei Ye^{1,4}, Nai-Qian Dong^{1,4}, Yi Kan^{1,4}, Yi-Bing Yang^{1,2}, Huai-Yu Zhao^{1,3}, Hong-Xiao Yu^{1,3}, Zi-Qi Lu^{1,5}, Jie-Jie Lei^{1,3}, Ben Liao^{1,5}, Xiao-Rui Mu^{1,3}, Ying-Jie Cao^{1,3}, Liangxing Guo², Jin Gao^{1,3}, Ji-Fu Zhou^{1,3}, Kai-Yang Yang^{1,3}, Hong-Xuan Lin^{1,3,4,5}✉ & Youshun Lin²✉

Soil alkalinization and global warming are predicted to pose major challenges to agriculture in the future, as they continue to accelerate, markedly reducing global arable land and crop yields^{1,2}. Therefore, strategies for future agriculture are needed to further improve globally cultivated, relatively high-yielding Green Revolution varieties (GRVs) derived from the *SEMIDWARF1 (SD1)* gene^{3,4}. Here we propose that precise regulation of the phytohormone gibberellin (GA) to optimal levels is the key to not only confer alkali-thermal tolerance to GRVs, but also to further enhance their yield. Endogenous modulation of *ALKALI-THERMAL TOLERANCE1/2 (ATT1/2)*, quantitative trait loci encoding GA20-oxidases or exogenous application of GA minimized rice yield loss affected by sodic soils. Mechanistically, high GA concentrations induce reactive oxygen species over-accumulation, whereas low GA concentrations repress the expression of stress-tolerance genes by means of DELLA-NGR5-mediated H3K27me3 methylation. We further showed that *ATT1* induces large fluctuations in GA levels, whereas *ATT2* is the ideal candidate for fine-tuning GA concentrations to appropriate levels to balance reactive oxygen species and H3K27me3 methylation to improve alkali-thermal tolerance and yield. Thus, *ATT2* is expected to be a potential new post-Green Revolution gene that could be harnessed to develop and use marginal lands for sustainable agriculture in the future.

The Green Revolution of the 1960s sharply increased agricultural production of cereal crops to ensure global food security^{5–8}. In the past few decades, Green Revolution varieties (GRVs) have been widely grown globally, because their semidwarf plant architecture confers lodging resistance under high-nitrogen fertilizer supply and reduces yield loss caused by wind and rain^{3,4,6}. The rice *SEMIDWARF1 (SD1)* gene encodes GA20-oxidase, a gibberellin (GA) biosynthesis enzyme⁹. Rice GRVs are characterized by a partial loss-of-function *sd1* allele encoding a defective GA20-oxidase enzyme that leads to a decrease in bioactive GA concentration, thus preventing the proteasomal degradation of SLENDER RICE1 (SLR1, the DELLA protein in rice) by the GA receptor GIBBERELLIN INSENSITIVE DWARF1 (GID1)^{9–12}. GAs comprise a class of tetracyclic diterpenoid phytohormones that are involved in regulating not only plant height, panicle length, spikelet number and growth-metabolism, but also regulate the response to adverse environments in rice^{3,4,13–18}. However, it is not clear how GA signals modulate the balance between crop yield and stress tolerance.

Soil salinization is a severe global issue that is aggravated by the rapidly changing climate. According to statistics from the Food and Agriculture Organization of the United Nations in 2021, more than 1.1 billion hectares of arable land worldwide is affected by salinity and sodicity, and about 40% are sodic fields (for example, high pH and

sodium (NaHCO_3 and Na_2CO_3) levels)¹⁹. Furthermore, it has been estimated that the global human population is increasing rapidly and will reach 11 billion by the year 2100²⁰. Rapid population increase and human activities are exacerbating the effects of climate change. Global average temperatures have risen by 1.2 °C since 1900 and will continue to increase in the next decade²¹, which will be devastating to agricultural production, contributing to reduced crop yields²². Global warming, in turn, has further intensified the sodification of cropland, resulting in a serious threat to world food security. Therefore, it is urgent that we develop new GRVs that integrate stress resilience and high yield to meet the demands of future population growth and climate change. However, little is known about how natural quantitative trait loci (QTL) confer alkali-thermal tolerance and yield traits in rice^{1,2,23–25}. In this study, based on the functional characterization of two QTL for alkali-thermal tolerance and yield traits in rice, we have discovered and proposed a previously unknown concept: maintaining moderate bioactive GA levels in rice either by endogenous genetic manipulation or by exogenous application of GA is the key to further increase the yield of GRVs while conferring multiple stress tolerance. Notably, we also found that only a slight increase in GA concentration in the GRVs allowed for marked yield increases in GRVs grown in normal fields and minimize yield losses in GRVs cultivated on sodic soils and under

¹National Key Laboratory of Plant Molecular Genetics, CAS Center for Excellence in Molecular Plant Sciences, Shanghai Institute of Plant Physiology and Ecology, Chinese Academy of Sciences, Shanghai, China. ²Shanghai Collaborative Innovation Center of Agri-Seeds, Joint Center for Single Cell Biology, School of Agriculture and Biology, Shanghai Jiao Tong University, Shanghai, China.

³University of the Chinese Academy of Sciences, Beijing, China. ⁴Guangdong Laboratory for Lingnan Modern Agriculture, Guangzhou, China. ⁵School of Life Science and Technology, ShanghaiTech University, Shanghai, China. ⁶These authors contributed equally: Shuang-Qin Guo, Ya-Xin Chen. ✉e-mail: hxlin@cemps.ac.cn; linyoushun@sjtu.edu.cn

heat-stress conditions, thus providing promising breeding strategies for future sustainable agriculture.

ATT1/2 confer alkali-thermal tolerance

To map the potential QTL that contribute to alkali and heat tolerance in rice, we constructed a set of chromosome segment substitution lines (CSSLs) using BART (*Oryza barthii*, a wild African rice species) as the donor parent and LTP ('Longtepu', *Oryza sativa* ssp. *indica*) as the recurrent parent for evaluation assays. Two lines (BA5 and BA17) that harboured single chromosomal segments from *O. barthii* on chromosomes 1 and 3, respectively, were sensitive to alkali and heat stress, suggesting that these segments carried QTL, namely *ATT1* (*ALKALI-THERMAL TOLERANCE 1*) and *ATT2*, that confer alkali-thermal tolerance in rice (Fig. 1a,b and Extended Data Fig. 1a–c). We further performed high-resolution mapping and narrowed the *ATT1* locus to a region of 174.75 kilobases (kb) containing 21 genes, 20 of which showed sequence variations in their genomic DNA. Similarly, the *ATT2* locus was narrowed to a 47.25-kb region that includes 18 genes, 16 of which showed variations in their genomic DNA sequence (Fig. 1a,b, Extended Data Fig. 1d–i and Supplementary Tables 1–6). We then generated near-isogenic lines (NILs) carrying the *ATT1* and *ATT2* loci of *O. barthii* by backcrossing with LTP (NIL-*ATT1*^{BART} and NIL-*ATT2*^{BART}). Under alkali and heat-stress conditions, both NIL-*ATT1*^{BART} or NIL-*ATT2*^{BART} were less tolerant than the isogenic controls NIL-*ATT1*^{LTP} or NIL-*ATT2*^{LTP} (Fig. 1c–h), indicating that *ATT1* and *ATT2* loci are involved in rice alkali-thermal tolerance.

The *ATT1* and *ATT2* chromosomal regions contain genes encoding GA20-oxidase 2 (*LOC_Os01g66100*) and GA20-oxidase 1 (*LOC_Os03g63970*), respectively (Supplementary Tables 1 and 2), which have been reported to regulate grain yield and abiotic stress in rice^{3,4,13,14,16–18}. We therefore inferred that *LOC_Os01g66100* and *LOC_Os03g63970* are the candidate genes for *ATT1* and *ATT2*, respectively. Sequence analysis of the promoter regions of the NILs showed that *ATT1* had 55 base differences and *ATT2* had 12 base differences, including single-base substitutions as well as single- and multiple-base insertions and deletions. We also found that the coding region of *ATT1* contained four nonsense mutations whereas *ATT2* had no mutations in the coding region (Supplementary Tables 7 and 8), suggesting that DNA sequence differences in the promoter regions could alter gene expression levels and confer alkali-thermal tolerance in rice. To test our hypothesis, we performed quantitative PCR with reverse transcription (RT-qPCR), and found that under normal conditions, the expression of *ATT1*^{BART} was higher than that of *ATT1*^{LTP}, and conversely, the expression of *ATT2*^{BART} was lower than that of *ATT2*^{LTP} (Extended Data Fig. 1j–m). However, the transcription of *ATT1* and *ATT2* was suppressed in response to alkali and high temperature stresses (Extended Data Fig. 1j–m).

We generated the loss-of-function mutants *att1* and *att2* using CRISPR-Cas9 gene editing and the overexpression lines OE-*ATT1* and OE-*ATT2* (Extended Data Fig. 2a,b and Supplementary Table 9). Compared with wild-type (WT) rice cultivars ('Nipponbare' (NIP) or 'Zhonghua 11' (ZH11)), *att1*, *att2* and OE-*ATT1* plants were sensitive to alkali and heat treatments, whereas OE-*ATT2* plants were more tolerant of alkali-thermal stresses (Fig. 1i–l and Extended Data Fig. 2c–j). Furthermore, genetic complementation showed that the transgenic lines containing *ATT1* genomic DNA from NIL-*ATT1*^{BART} in NIL-*ATT1*^{LTP} background (*gATT1*^{BART}/NIL-*ATT1*^{LTP}) showed reduced alkali-thermal tolerance compared to NIL-*ATT1*^{LTP} plants; knocking out of *ATT1* in NIL-*ATT1*^{BART} (*att1*/NIL-*ATT1*^{BART}) resulted in increased alkali-thermal tolerance compared to NIL-*ATT1*^{BART} plants (Fig. 1m, Extended Data Fig. 2k,m,n,q–s and Supplementary Table 9). The complementary lines containing *ATT2* genomic DNA from NIL-*ATT2*^{LTP} in NIL-*ATT2*^{BART} background (*gATT2*^{LTP}/NIL-*ATT2*^{BART}) showed enhanced alkali-thermal tolerance compared to NIL-*ATT2*^{BART} plants; knocking out of *ATT2*

in NIL-*ATT2*^{LTP} (*att2*/NIL-*ATT2*^{LTP}) led to a decrease in alkali-thermal tolerance compared to NIL-*ATT2*^{LTP} plants (Fig. 1n, Extended Data Fig. 2l,o,p,t–v and Supplementary Table 9). Taken together, these results confirm that *ATT1* and *ATT2* are the QTL responsible for alkali-thermal tolerance in rice.

ATT1/2 control GA for stress tolerance

GA₂₀ and GA₉, products of the GA20-oxidases *ATT1* and *ATT2*, are converted to the bioactive GA species GA₁ and GA₄ in the early-13-hydroxylation pathway (GA₁ pathway) and the non-13-hydroxylation pathway (GA₄ pathway), respectively^{17,26,27} (Fig. 2a). Therefore, we performed quantitative analyses using rice seedlings and showed that the endogenous levels of GA₁, GA₄, GA₁₉, GA₂₄, GA₂₀ and GA₉ were increased in NIL-*ATT1*^{BART} and decreased in NIL-*ATT2*^{BART} plants compared with LTP (NIL-*ATT1*^{LTP}/NIL-*ATT2*^{LTP}) (Fig. 2a). Furthermore, compared with WT (NIP or ZH11), the *att1* and *att2* mutants showed lower levels of GA₁ and GA₄, whereas the OE-*ATT1* or OE-*ATT2* transgenic plants showed high or slightly higher levels of GA₁ and GA₄ (Fig. 2b), which was due to higher enzyme activity of *ATT1* than *ATT2* (Extended Data Fig. 3a–c). Notably, *att1*/*att2* double mutant plants had the lowest levels of GA₁ and GA₄ (Fig. 2b). These results indicate that *ATT1* and *ATT2* may function to modulate levels of bioactive GA and contribute to rice alkali-thermal tolerance.

Next, we conducted tissue-specific expression analysis, revealing that *ATT1* was predominantly expressed in leaves, whereas *ATT2* was mainly expressed in stems and panicles under normal conditions (Extended Data Fig. 3d,e). Notably, both alkali and heat stresses did not alter the expression patterns of *ATT1* and *ATT2* (Extended Data Fig. 3e). To further show the kinetic response of *ATT1* and *ATT2* in regulating GA biosynthesis under alkaline and heat stress, we performed quantitative analyses of bioactive GAs in rice plants at the booting stage. The results indicated that NIL-*ATT1*^{BART} had higher and NIL-*ATT2*^{BART} had lower levels of bioactive GAs compared to NIL-*ATT1*^{LTP}/NIL-*ATT2*^{LTP} in all three tissues (stems, leaves and panicles) under normal conditions as well as alkali and heat stress. Furthermore, we found that bioactive GAs accumulated most abundantly in panicles compared to stems and leaves, which did not align with the tissue expression patterns of *ATT1* and *ATT2* (Fig. 2c and Extended Data Fig. 3d–f). This discrepancy may be attributed to the localized transport of GA depending on plant development and response to ambient environment^{28,29}. Furthermore, we observed that alkali and heat stresses gradually repressed the accumulation of bioactive GAs in stems, leaves and panicles (Fig. 2c and Extended Data Fig. 3f). Given that the expression of GA biosynthesis genes, *ATT1* and *ATT2*, was repressed under alkali and heat stresses (Extended Data Fig. 1j–m), we also examined the expression of GA catabolism genes, that is, *OsGA2oxs* and *EUII*, and found that they were mostly upregulated under alkali and heat stresses (Extended Data Fig. 3g,h), leading to decreased levels of bioactive GAs.

To further investigate the correlation between bioactive GA and alkali-thermal tolerance, we exogenously applied bioactive GA (GA₃) to LTP plants and observed that the application of 0.1 μM bioactive GA significantly improved alkali-thermal tolerance in seedlings (Fig. 3a–c and Extended Data Fig. 4a–c). By contrast, seedlings treated with 1 or 10 μM concentrations of GA or paclobutrazol (PAC, a GA biosynthesis inhibitor) were sensitive to both alkali and heat stress (Fig. 3d–f). Provided that NIL-*ATT1*^{BART}, LTP (NIL-*ATT1*^{LTP}/NIL-*ATT2*^{LTP}) and NIL-*ATT2*^{BART} plants contained high, medium and low levels of endogenous bioactive GA, respectively (Fig. 2a), we further found that, in contrast to NIL-*ATT1*^{BART} and LTP, NIL-*ATT2*^{BART} was more tolerant of alkali-thermal stresses when GA was exogenously applied to either the roots (Fig. 3g and Extended Data Fig. 4d,e) or leaves (Extended Data Fig. 4h–j). Consistently, NIL-*ATT1*^{BART} (high GA level) was more tolerant of alkali-thermal stresses than NIL-*ATT2*^{BART} (low GA level) and LTP (medium GA level) when PAC was exogenously applied (Fig. 3h and Extended

Article

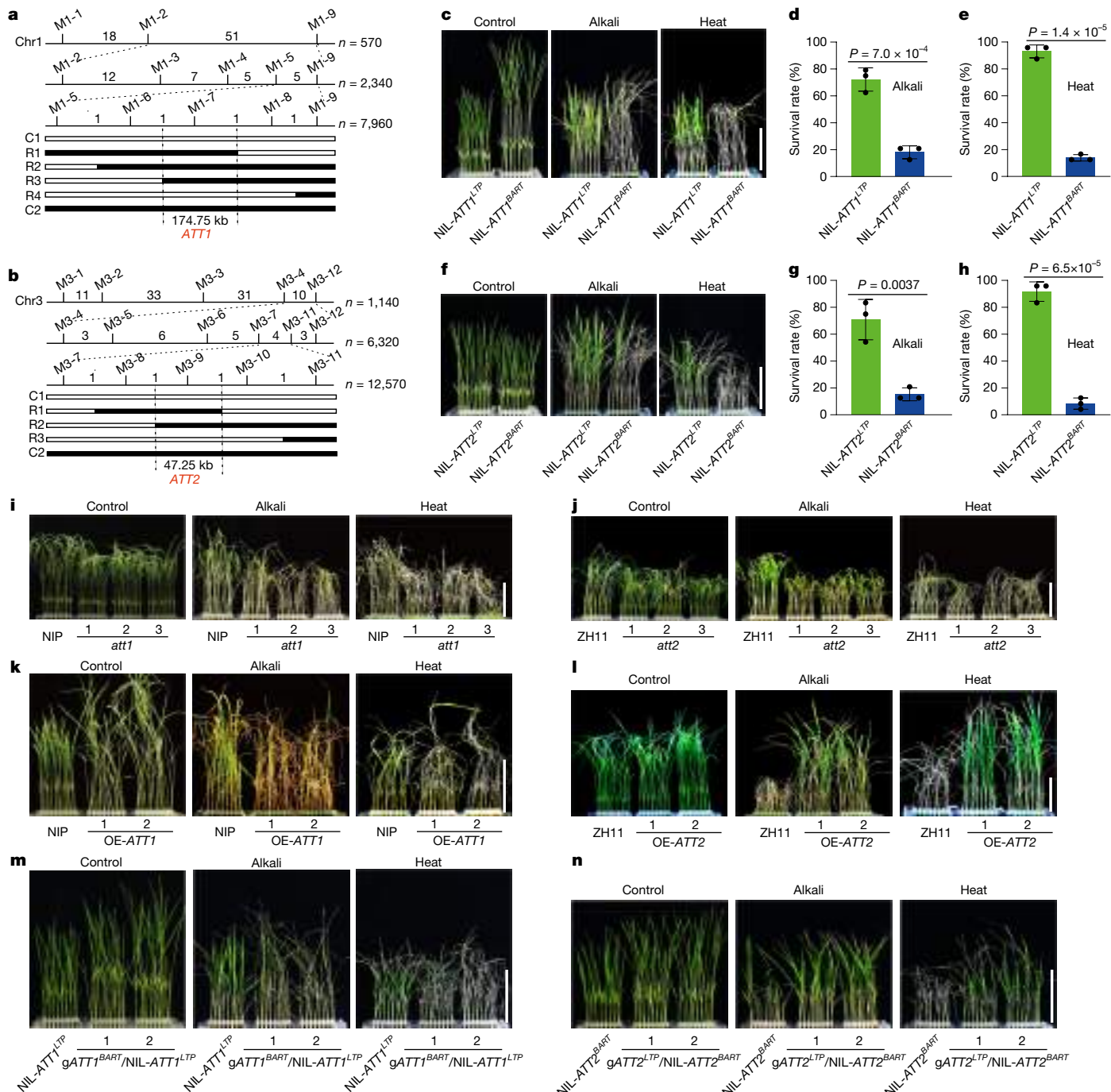


Fig. 1 | Identification of the ATT1 and ATT2 loci for alkali-thermal tolerance in rice. **a,b**, Map-based cloning of ATT1 (**a**) and ATT2 (**b**). The numbers between the molecular markers represent the number of recombinants, and *n* represents total number of individual plants. The white and black bars represent chromosomal segments from LTP and BART, respectively. R1-R4 in **a** and R1-R3 in **b** indicate homozygous recombinant segments. ATT1 was mapped to a 174.75-kb region between markers M1-6 and M1-8 on chromosome 1, and ATT2 was mapped to a 47.25-kb region between markers M3-8 and M3-10 on chromosome 3. **c-h**, Phenotypes (**c,f**) and survival rates (**d,e,g,h**) of NIL-ATT1^{LTP} and NIL-ATT1^{BART} (**c-e**) and NIL-ATT2^{LTP} and NIL-ATT2^{BART} (**f-h**) plants.

In **d,e,g,h**, data are mean ± s.d.; *n* = 3, biologically independent samples, each sample consisted of 24 seedlings. Two-tailed Student's *t*-tests were used to determine *P* values. **i-n**, Phenotypes of *att1* mutant (**i**), *att2* mutant (**j**), overexpression-ATT1(OE-ATT1) (**k**), overexpression-ATT2(OE-ATT2) (**l**) transgenic plants and gATT1^{BART}/NIL-ATT1^{LTP} (**m**) and gATT2^{LTP}/NIL-ATT2^{BART} (**n**) complementary lines. Alkali treatment, 65 mM sodium bicarbonate; **c,d,f,g,m,n**, 14 days; **i-k**, 10 days; **l**, 11 days. Heat treatment, 42 °C and RH > 90%; **c,e,f,h,m,n**, 28 h; **i-k**, 20 h; **l**, 22 h. 12-day-old plants were subjected to stress treatments and then recovered for 7 days. Scale bars, 10 cm (**c,f,i-n**).

Data Fig. 4f,g). These results indicate that the maintenance of a proper level of active GA can improve alkali-thermal tolerance in rice.

Furthermore, we performed phenotypic evaluations using rice lines or varieties that contain a range of endogenous levels of active GAs (Fig. 2b). The *att1* (low GA level), *att2* (low GA level) and *att1/att2* (lowest

GA level) mutants were less tolerant of alkali-thermal stresses than the WT controls (NIP or ZH11 containing medium levels of GA) (Figs. 1i,j, 2b, 3i-k and Extended Data Fig. 2c-f). Among them, the *att1/att2* plants (lowest GA level) were even more sensitive than *att1* plants (low GA level) (Figs. 2b and 3i-k). Consistently, NIL-ATT1^{93II} plants (low GA level)

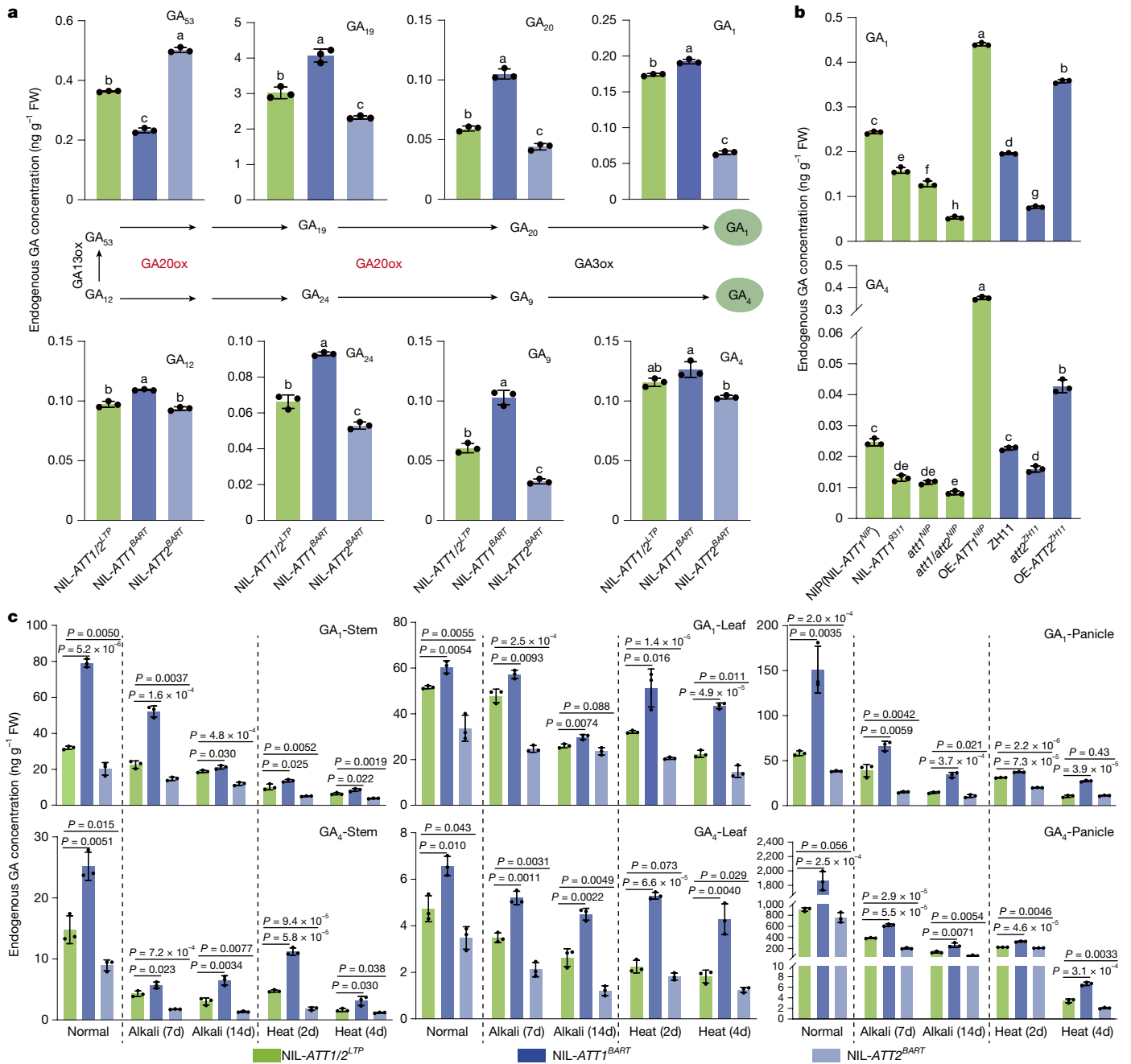


Fig. 2 | ATT1 and ATT2 modulate GA synthesis. **a**, Endogenous GA levels in NIL-ATT1/2^{LTP} (NIL-ATT1^{LTP}/ATT2^{LTP}), NIL-ATT1^{BART} and NIL-ATT2^{BART} seedlings and a schematic diagram of the GA₁ and GA₄ synthesis pathways. FW, fresh weight; ox, -oxidase. **b**, GA₁ and GA₄ contents in NIP (NIL-ATT1^{NIP}), NIL-ATT1^{93II}, att1^{NIP}, att1/att2^{NIP}, OE-ATT1^{NIP}, ZH11, att2^{ZH11} and OE-ATT2^{ZH11} seedlings. **c**, Endogenous GA of GA₁ and GA₄ levels in stems, leaves and panicles of NIL-ATT1/2^{LTP} (NIL-ATT1^{LTP}/ATT2^{LTP}), NIL-ATT1^{BART} and NIL-ATT2^{BART} plants at the booting stage under normal

conditions, alkali and heat treatments. Alkali treatment, 150 mM sodium bicarbonate for 7 or 14 days (7d, 14d, respectively); heat treatment, 45°C and RH > 90% for 2 or 4 days (2d, 4d, respectively). Data are mean \pm s.d.; $n = 3$, biologically independent samples. In **a** and **b**, the same lower-case letters above the bars indicate no significant difference at $P > 0.05$ as determined by two-way analysis of variance (ANOVA) with a least-significant difference (LSD) test. In **c**, two-tailed Student's *t*-tests were used to determine *P* values.

were more sensitive to heat and alkali than NIL-ATT1^{NIP} plants (medium GA level) (Fig. 2b and Extended Data Fig. 4k–m). ‘Nanjing’ (NJ6) is a variety that contains high GA levels, and the mutation of ATT1 in NJ6 restored endogenous GA to medium levels (Extended Data Fig. 4n). In addition, we tested *gid1* (GIBBERELLIN INSENSITIVE DWARF1; GID1) mutant plants, in which GA signalling is blocked^{3,4}. Consistently, *att1* (NJ6) was found to be more tolerant of alkali–thermal treatments compared with NJ6 and *gid1* plants (Fig. 3l–n). Furthermore, the *att2* (NJ6) was more tolerant to alkali–thermal stresses compared to NJ6 and *att1* (NJ6), whereas the *att1/att2* (NJ6) mutant was less tolerant to

alkali–thermal stresses compared to *att1* (NJ6) and *att2* (NJ6) (Fig. 3o–q and Supplementary Table 9). The OE-ATT2 (NJ6) was more sensitive to alkali–thermal stresses than NJ6 (Fig. 3r–u). In summary, these results support the new concept that maintaining appropriate levels of bioactive GAs is the key to improving stress tolerance in rice.

High GA levels enhance ROS accumulation

Previous studies have shown that high endogenous GA levels reduce the abundance of DELLA, which triggers the accumulation of reactive

Article

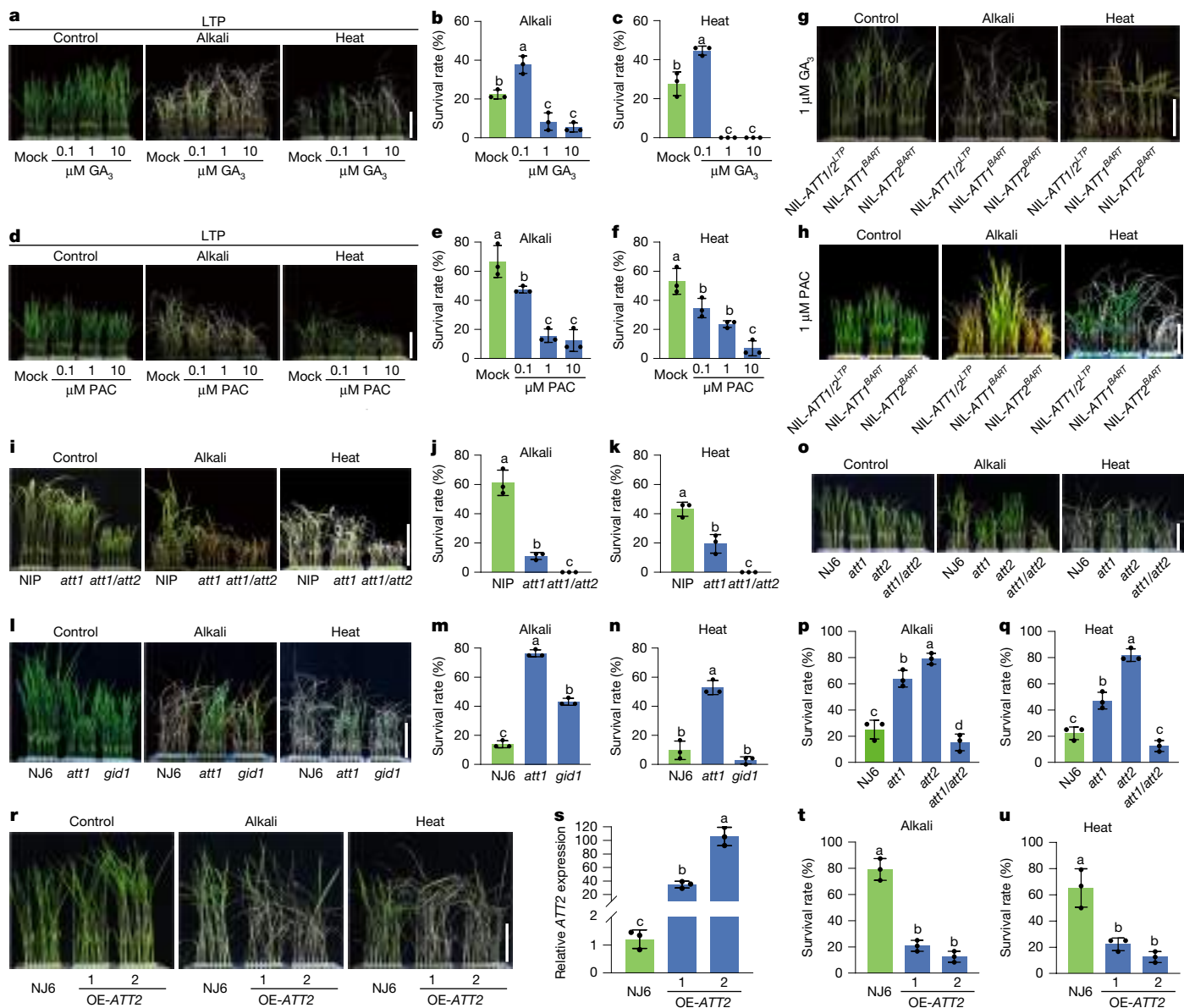


Fig. 3 | GA levels regulate alkali-thermal tolerance. **a–f**, Phenotypes (**a,d**) and survival rates (**b,c,e,f**) of 12-day-old LTP seedlings treated with various concentrations of GA (**a–c**) and PAC (**d–f**). **g,h**, Phenotypes of NIL-ATT1^{LTP} (NIL-ATT1^{LTP}/ATT2^{LTP}), NIL-ATT1^{BART} and NIL-ATT2^{BART} plants in response to 1 μM GA (**g**) and 1 μM PAC (**h**) treatments on root. **i–n**, Phenotypes (**i,l**) and survival rates (**j,k,m,n**) of the att1 and att1/att2 mutants in the NIP background (**i–k**), and the att1 and gid1 mutants in the NJ6 background (**l–n**). **o–r**, Phenotypes (**o,r**) and survival rates (**p,q,t,u**) of the att1, att2 and att1/att2 mutants and OE-ATT2 in the NJ6 background, and the ATT2 expression levels (**s**) of OE-ATT2

lines in NJ6 background. Alkali treatment, 65 mM sodium bicarbonate for 14 days (**a–h**) or 10 days (**i,j**), 12 days (**l–q**) and 11 days (**r,t,u**); Heat treatment, 42 °C and RH > 90% for 28 h (**a–h**), 20 h (**i,k**), 24 h (**l–q**) and 23 h (**r,t,u**); 12-day-old seedlings were subjected to stress treatments and then recovered for 7 days. In **b,c,e,f,j,k,m,n,p,q,s–u**, data are mean \pm s.d.; $n = 3$, biologically independent samples, each sample consisted of 24 seedlings. The same lowercase letters indicate no significant difference at $P > 0.05$ as determined by two-way ANOVA with LSD test. Scale bars, 10 cm (**a,g,d,h,i,o,l,r**).

oxygen species (ROS)^{30,31}. Consistently, the abundance of SLR1 (DELLA protein in rice) was lower in NIL-ATT1^{BART} plants (high GA level) compared to the isogenic control NIL-ATT1^{LTP} (medium GA level) (Figs. 2a, 4a and Extended Data Fig. 5a). To explore the molecular mechanism behind the ATT1 and ATT2 regulation of alkali-thermal tolerance, we examined ROS levels in the NILs that contain different GA concentrations. We found that stress-induced ROS accumulation and the ROS contents of NIL-ATT1^{LTP} plants (medium GA level) were significantly lower than that of NIL-ATT1^{BART} plants (high GA level) under normal conditions and alkaline and heat treatments, indicating that NIL-ATT1^{LTP} plants may be effective at eliminating ROS to confer stress tolerance compared with NIL-ATT1^{BART} plants (Figs. 1c–e, 4b

and Extended Data Fig. 5b). To verify our hypothesis, we measured the enzymatic activity of peroxidase (POX, an H₂O₂ scavenger). POX activity in the NIL-ATT1^{LTP} plants (medium GA level) was higher than in the NIL-ATT1^{BART} plants (high GA level) in the control, alkaline and heat treatments (Extended Data Fig. 5c). However, NIL-ATT2^{BART} plants (low GA level) that accumulate high levels of SLR1 contained low levels of H₂O₂ compared to NIL-ATT2^{LTP} (medium GA level), yet were still highly sensitive to alkaline and heat stresses, indicating that the stress sensitivity of NIL-ATT2^{BART} plants was not caused by H₂O₂ accumulation (Figs. 1f–h, 2a and 4c,d; next section).

We next examined the expression of key genes that encode antioxidants that protect cells from stress-induced oxidative damage^{1,32}, such

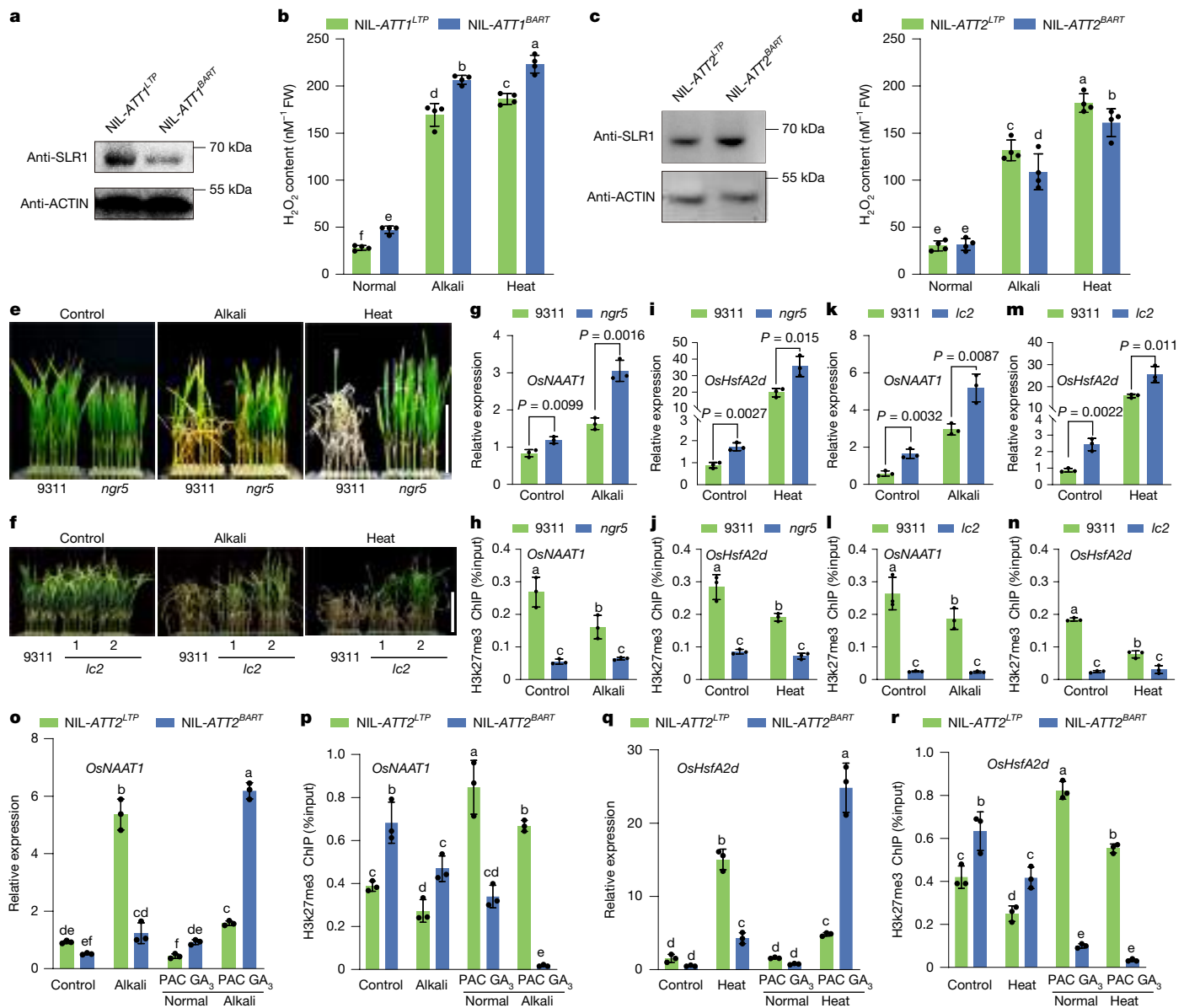


Fig. 4 | Modulation of ROS concentrations and H3K27me3 levels by ATT1 and ATT2 to control alkali-thermal tolerance. **a**, Immunodetection of SLR1 in NIL- $ATT1^{LTP}$ and NIL- $ATT1^{BART}$ plants. Actin was the loading control. The experiment was repeated independently three times with similar results. **b**, H_2O_2 content in NIL- $ATT1^{LTP}$ and NIL- $ATT1^{BART}$ plants. **c**, Immunodetection of SLR1 in NIL- $ATT2^{LTP}$ and NIL- $ATT2^{BART}$ plants. Actin was the loading control. The experiment was repeated independently three times with similar results. **d**, H_2O_2 content in NIL- $ATT2^{LTP}$ and NIL- $ATT2^{BART}$ plants. **e,f**, Phenotypes of *ngr5* mutant plants (**e**) and *lc2* mutant lines (**f**) compared to 9311 (WT). Alkali treatments, 65 mM sodium bicarbonate for 12 days; heat treatments, 42 °C, RH > 90% for 24 h; 12-day-old plants were subjected to stress treatments and then recovered for 7 days. **g–j**, Comparisons of mRNA abundance (**g,i**) and H3K27me3 modification (**h,j**) for *OsNAAT1* (**g,h**) and *OsHsfA2d* (**i,j**) between the

9311 and *ngr5* mutant plants. **k–n**, Comparisons of mRNA abundance (**k,m**) and H3K27me3 modification (**l,n**) for *OsNAAT1* (**k,l**) and *OsHsfA2d* (**m,n**) between the 9311 and *lc2* mutant plants. **o–r**, Comparisons of mRNA abundance (**o,p**) and H3K27me3 modification (**p,r**) for *OsNAAT1* (**o,p**) and *OsHsfA2d* (**q,r**) between NIL- $ATT2^{LTP}$ and NIL- $ATT2^{BART}$ plants treated with 0.1 μ M GA₃ or 0.1 μ M PAC before alkali and heat treatments. Alkali treatments, 65 mM sodium bicarbonate for 24 h; heat treatments, 42 °C, RH > 90% for 3 h; 12-day-old plants were subjected to stress treatments. In **b,d,g–r**, data are mean \pm s.d.; $n = 3$, biologically independent samples. In **g,i,k,m**, two-tailed Student's *t*-tests were used to determine *P* values. In **b,d,h,j,l,n–r**, the same lower-case letters indicate no significant difference at $P > 0.05$ as determined by two-way ANOVA with LSD test. Scale bars, 10 cm (**e,f**).

as ascorbate POX (APX), superoxide dismutase and catalase (CAT). We found that these genes were upregulated in response to alkali and heat treatments, and that expression was significantly higher in NIL- $ATT1^{LTP}$ plants (medium GA level) compared to NIL- $ATT1^{BART}$ plants (high GA level) (Extended Data Fig. 5d–j). Taken together, appropriate levels of active GAs in NIL- $ATT1^{LTP}$ plants enhanced the capability of antioxidant systems, thereby alleviating the stress-induced ROS over-accumulation and thus conferring alkali-thermal tolerance in rice.

Low GA levels enhance H3K27me3

Although NIL- $ATT2^{BART}$ plants (low GA level) accumulated more SLR1 and less H_2O_2 than did NIL- $ATT2^{LTP}$ plants (medium GA level), they still showed extreme sensitivity to alkaline and heat stress (Figs. 1f–h, 4c,d and Extended Data Fig. 5a). To explore the underlying mechanisms, we conducted RNA sequencing (RNA-seq) analysis and found that *ATT2* overexpression led to increased numbers of upregulated genes in OE-*ATT2* (optimal medium GA level) compared with ZH11 (medium GA

level; WT control) in the control, alkaline, and heat treatments (Fig. 2b and Extended Data Fig. 6a). Thus, we speculated that epigenetic repression of gene expression in OE-*ATT2* plants may be relieved compared to ZH11. A previous study reported that GAs promoted SLR1 (DELLA) degradation and transcription factor NGR5 (NITROGEN-MEDIATED TILLER GROWTH RESPONSE 5) instability. Moreover, NGR5 recruited leaf inclination 2 (LC2, a component of the polycomb repressor complex 2) to mediate transcriptional reprogramming by histone H3 lysine 27 tri-methylation (H3K27me3)³. We reasoned that H3K27me3 could potentially be involved in rice alkali-thermal tolerance. Phenotypic analysis showed that *ngr5* and *lc2* mutant plants were more tolerant of alkaline and heat stress compared to the WT controls (9311) (Fig. 4e, f, and Extended Data Fig. 6b–g). Conversely, OE-*NGR5* and OE-*LC2* plants were more sensitive to alkaline and heat stresses than the WT plants (Extended Data Fig. 6h–o), indicating that H3K27me3 negatively regulates alkali-thermal tolerance in rice.

To further explore the causal genes modified by H3K27me3 that confer alkali-thermal tolerance in rice, we next analysed the transcriptome profiles of OE-*ATT2* and ZH11 plants and found two genes of particular interest: *OsNAAT1* (nicotianamine aminotransferase 1) and *OsHsfA2d*, which were highly expressed in response to alkaline and heat stresses, respectively (Extended Data Fig. 7a–d). In alkaline soils, NAAT1 synthesizes chelating agents to solubilize and enhance iron (Fe) uptake, thereby improving the tolerance of crop plants to low Fe availability in alkaline soils³³. *OsHsfA2d* encodes a master heat-shock transcription factor (HSF) that regulates high temperature tolerance through the activation of JASMONATE ZIM-DOMAIN proteins and many heat-shock proteins³⁴. To test whether *OsNAAT1* and *OsHsfA2d* were modified by H3K27me3 by means of NGR5 and LC2, we performed chromatin immunoprecipitation with real-time qPCR (ChIP-qPCR) and electrophoretic mobility shift assays (EMSA), which showed that NGR5-HA binds directly to the gene coding regions of *OsNAAT1* and *OsHsfA2d* (Extended Data Fig. 7e–h). In addition, we found that *naat1* (*OsNAAT1* mutant) plants were sensitive to alkali treatment and that *hsfa2d* (*OsHsfA2d* mutant) plants were sensitive to heat treatment (Extended Data Fig. 7i–l). Consistently, in the control, alkaline and heat treatments, the relative abundances of *OsNAAT1*- and *OsHsfA2d*-specific messenger RNAs (mRNAs) were significantly higher in the *ngr5* and *lc2* mutant plants than in WT; conversely, the levels of H3K27me3 modification in the *OsNAAT1* and *OsHsfA2d* genes were decreased accordingly in the *ngr5* and *lc2* mutants compared to WT (Fig. 4g–n). Furthermore, *OsNAAT1* and *OsHsfA2d* showed lower transcript levels and higher H3K27me3 modifications levels in NIL-*ATT2^{BART}* plants (low GA level) than in NIL-*ATT2^{LTP}* plants (medium GA level), and this phenomenon could be reversed by exogenous application of bioactive GAs (GA₃) or a GA inhibitor (PAC) (Fig. 4o–r). In conclusion, these results indicate that low levels of GAs increase the abundance of SLR1 (DELLA) and suppress the expression of alkali- and heat-inducible tolerance genes by means of SLR1-NGR5-LC2-mediated H3K27me3 modification, leading to susceptibility to environmental stresses in rice.

Medium GA enhances yield and tolerance

Medium levels of bioactive GAs enhance stress tolerance in rice (Figs. 1c–l and 2); however, the precise association between GA concentration and grain yield is unclear. Since the levels of bioactive GAs are controlled by *ATT1* and *ATT2*, we were able to evaluate the yield traits of the NIL-*ATT1^{LTP}*/NIL-*ATT1^{BART}*, NIL-*ATT1^{NIP}*/NIL-*ATT1⁹³¹¹* and NIL-*ATT2^{LTP}*/NIL-*ATT2^{BART}* plants under normal field conditions. Field trials showed that NIL-*ATT1^{LTP}*, NIL-*ATT1^{NIP}* and NIL-*ATT2^{LTP}* plants had grain yield increases of 40.91, 94.86 and 19.50% per plant and increases of 29.89, 40.87 and 15.42% in grain yield per plot compared to the isogenic controls NIL-*ATT1^{BART}*, NIL-*ATT1⁹³¹¹* and NIL-*ATT2^{BART}* in Shanghai, respectively (Fig. 5a–c and Extended Data Fig. 8a–h). Furthermore,

NIL-*ATT1^{LTP}* and NIL-*ATT2^{LTP}* plants had grain yield increases of 36.51 and 31.23% per plant and increases of 28.70 and 21.10% in grain yield per plot compared to the isogenic controls NIL-*ATT1^{BART}* and NIL-*ATT2^{BART}* in Hainan, respectively (Extended Data Fig. 8i–s). In addition, *att1/att2* mutant showed a marked decrease in plant height and grain yield per plant compared with the *att1* and *att2* mutants and the WT plants, indicating that *ATT1* and *ATT2* have additive genetic effects (Extended Data Fig. 9). Notably, overexpression of *ATT2* (optimal medium GA level) in ZH11, a Green Revolution semidwarf variety carrying a partially functional *SD1/ATT1* gene with medium GA level, resulted in a slight increase in endogenous bioactive GAs and further increased the yield of ZH11 by 22.66–30.88% per plant and by 18.77–20.35% per plot (Figs. 2b and 5d–f). The yield increase observed in OE-*ATT2* was primarily due to an increase in grain number per panicle (Extended Data Fig. 10a–h), consistent with our previous findings¹³. These results indicate that genetic manipulation of *ATT2* is promising to precisely regulate GAs at the optimal medium level, thereby further improving grain yield in high-yielding GRVs under normal field conditions.

Next, we investigated the contributions of GA on yield traits under alkali-thermal stresses. For alkaline stress, the NILs were planted throughout the growth stages in alkaline pools, simulating sodic fields, with the pH value maintained at around 9.0 (Extended Data Fig. 10i–l). Under alkaline conditions, NIL-*ATT1^{NIP}* plants (medium GA level) and NIL-*ATT2^{LTP}* plants (medium GA level) showed 59.03 and 25.88% increases in grain yield per plant and 39.47 and 26.05% increases in grain yield per plot, respectively, compared to their isogenic controls NIL-*ATT1⁹³¹¹* (low GA level) and NIL-*ATT2^{BART}* (low GA level) (Fig. 5g–i and Extended Data Fig. 11a–h). NIL-*ATT1^{LTP}* plants (medium GA level) had a 19.3% yield reduction per plant and an 8.17% decrease in grain yield per plot compared to the isogenic control NIL-*ATT1^{BART}* (high GA level) (Fig. 5g–i and Extended Data Fig. 11a–h). Consistently, under alkaline conditions, NIL-*ATT2^{LTP}* plants (31.55%) showed lower plot yield loss compared to the corresponding isogenic controls NIL-*ATT2^{BART}* (37.32%), whereas NIL-*ATT1^{LTP}* plants (32.29%) showed higher plot yield loss compared to the corresponding isogenic controls NIL-*ATT1^{BART}* (4.23%) (Extended Data Fig. 11i, j). Given that rice varieties with moderate GA levels are expected to achieve maximum yields, we therefore reasoned that alkaline stress may reduce endogenous GA concentrations in rice, with GA levels in NIL-*ATT1^{BART}* plants decreasing from high to near-medium and in NIL-*ATT1^{LTP}* plants from medium to low. This hypothesis was further supported by exogenous application of GAs, which alleviated the yield loss caused by alkaline stress in two high-yielding GRVs tested (Fig. 5j–m and Supplementary Table 10). We also evaluated the yield performance of overexpression of *ATT2* (optimal medium GA level) in ZH11 in alkaline soil and showed a 80.67–88.88% increase in grain yield per plant and a 77.96–100.92% increase in grain yield per plot compared with the ZH11 (medium GA level) (Fig. 5n–p and Extended Data Figs. 10n–p, 11k–r). The above results indicate that precise regulation of GAs to moderate levels, either endogenous or exogenous, can markedly enhance alkali tolerance and grain yield in rice exposed to alkaline conditions.

For heat stress, NILs at the grain-filling stage were treated in sunlight-heated greenhouses covered with plastic film to simulate heat stress in natural fields (Extended Data Fig. 10m). Under high temperature conditions in the field, NIL-*ATT1^{LTP}*, NIL-*ATT1^{NIP}* and NIL-*ATT2^{LTP}* plants with medium GA levels had 49.72, 51.51 and 41.52% higher grain yields per plant and 84.76, 31.38 and 23.65% higher grain yields per plot compared to the corresponding isogenic controls NIL-*ATT1^{BART}* (high GA level), NIL-*ATT1⁹³¹¹* (low GA level) and NIL-*ATT2^{BART}* (low GA level), respectively (Fig. 5q–s and Extended Data Fig. 12a–h). Consistently, under heat stress, NIL-*ATT1^{LTP}* (18.49%) and NIL-*ATT2^{LTP}* (12.26%) plants with medium GA levels showed lower plot yield losses compared to the corresponding isogenic controls NIL-*ATT1^{BART}* (42.70%) with high GA levels and NIL-*ATT2^{BART}* (18.10%) with low GA levels, respectively (Extended Data Fig. 12i, j). These data indicate that maintaining GA at

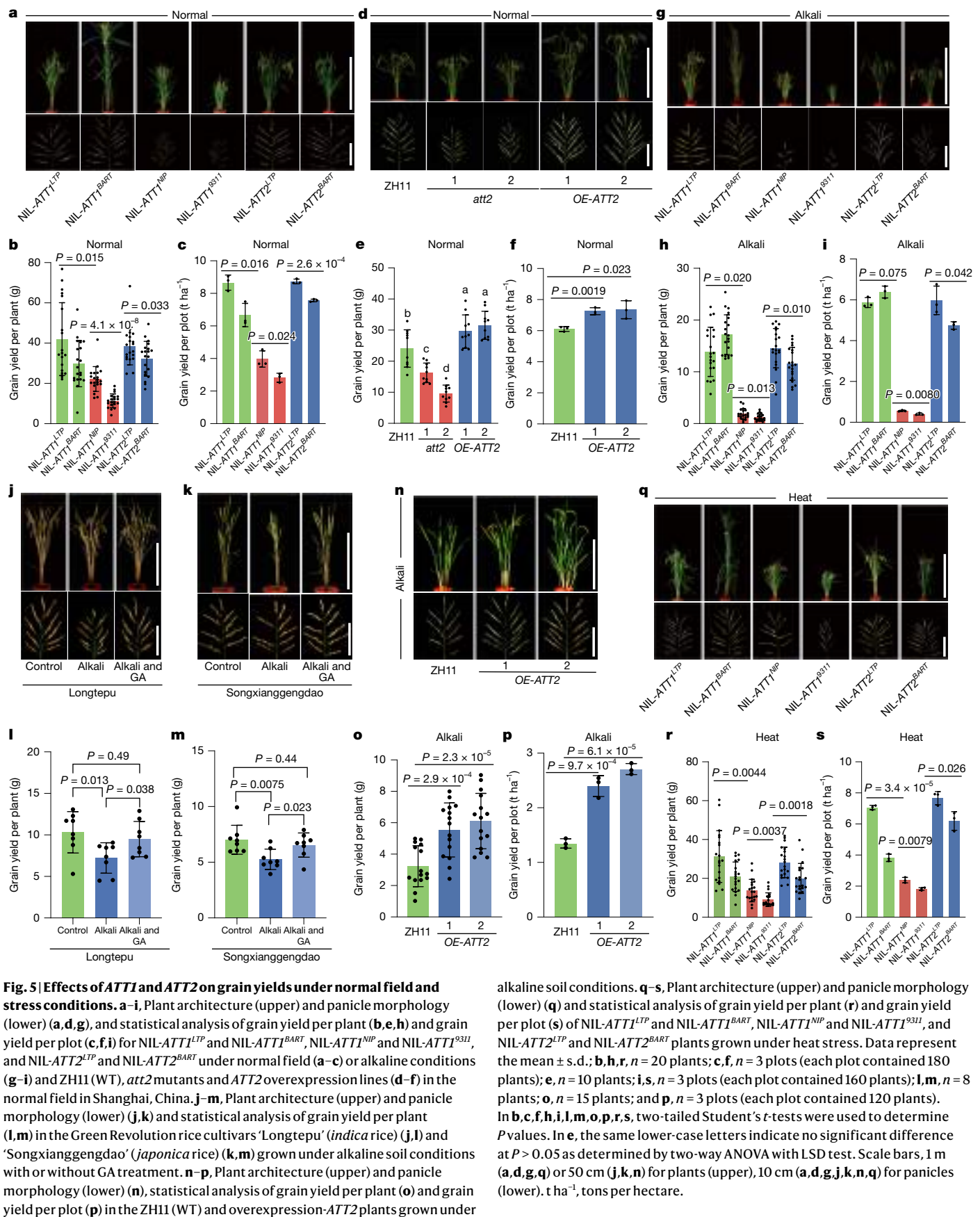


Fig. 5 | Effects of *ATT1* and *ATT2* on grain yields under normal field and stress conditions. **a–i**, Plant architecture (upper) and panicle morphology (lower) (**a,d,g**), and statistical analysis of grain yield per plant (**b,e,h**) and grain yield per plot (**c,f,i**) for NIL-*ATT1*^{LTP} and NIL-*ATT1*^{BART}, NIL-*ATT1*^{NP} and NIL-*ATT1*⁹³¹¹, and NIL-*ATT2*^{LTP} and NIL-*ATT2*^{BART} under normal field (**a–c**) or alkaline conditions (**g–i**) and ZH11 (WT). *att2* mutants and *ATT2* overexpression lines (**d–f**) in the normal field in Shanghai, China. **j–m**, Plant architecture (upper) and panicle morphology (lower) (**j,k**) and statistical analysis of grain yield per plant (**l,m**) in the Green Revolution rice cultivars ‘Longtepu’ (*indica* rice) (**j,l**) and ‘Songxianggengdao’ (*japonica* rice) (**k,m**) grown under alkaline soil conditions with or without GA treatment. **n–p**, Plant architecture (upper) and panicle morphology (lower) (**n**), statistical analysis of grain yield per plant (**o**) and grain yield per plot (**p**) in the ZH11 (WT) and overexpression-*ATT2* plants grown under

alkaline soil conditions. **q–s**, Plant architecture (upper) and panicle morphology (lower) (**q**) and statistical analysis of grain yield per plant (**r**) and grain yield per plot (**s**) of NIL-*ATT1*^{LTP} and NIL-*ATT1*^{BART}, NIL-*ATT1*^{NP} and NIL-*ATT1*⁹³¹¹, and NIL-*ATT2*^{LTP} and NIL-*ATT2*^{BART} plants grown under heat stress. Data represent the mean \pm s.d.; **b,h,r**, $n = 20$ plants; **c,f,i**, $n = 3$ plots (each plot contained 180 plants); **e,n**, $n = 10$ plants; **i,s**, $n = 3$ plots (each plot contained 160 plants); **l,m,o,p,r,s**, $n = 8$ plants; **o,n**, $n = 15$ plants; and **p,n**, $n = 3$ plots (each plot contained 120 plants). In **b,c,f,h,i,l,m,o,p,r,s**, two-tailed Student’s *t*-tests were used to determine *P* values. In **e**, the same lower-case letters indicate no significant difference at $P > 0.05$ as determined by two-way ANOVA with LSD test. Scale bars, 1 m (**a,d,g,q**) or 50 cm (**j,k,n**) for plants (upper), 10 cm (**a,d,g,j,k,n,q**) for panicles (lower). $t\text{ ha}^{-1}$, tons per hectare.

medium levels is beneficial to improving rice thermotolerance and mitigating the yield loss caused by heat stress.

Discussion

The Green Revolution hormone GA promotes the degradation of DELLA proteins, which restrains plant growth and the responses to adverse environmental conditions^{10,12,18,26}. However, the mechanistic insight into how GA balances development and stress tolerance to maximize crop yield under normal or stressed conditions remains elusive. In this study, we have proposed a previously unknown concept that precise regulation of GA at optimal medium levels is the preferred solution to confer high grain yield and tolerance to alkali–thermal stresses simultaneously (Extended Data Fig. 12k). High levels of GA triggered the degradation of DELLA, leading to excessive accumulation of ROS, which proved to be detrimental to plants, especially under environmental stress conditions^{30,31} (Extended Data Fig. 12k). Rice plants containing low levels of GA also showed high susceptibility to alkaline and heat stresses (Extended Data Fig. 12k). We found that the expression of stress-tolerance genes, such as *OsNAAT1* and *OsHsfA2d*, was repressed by SLR1/DELLA–NGR5-mediated modification of H3K27me3, which explains why rice plants with low GA levels were also highly sensitive to alkaline and heat stresses, despite the low ROS levels in these plants. Therefore, maintaining moderate GA levels is the key to balancing H3K27me3 modification levels and ROS concentrations to maximize stress tolerance and grain yield in rice (Extended Data Fig. 12k). The heterotrimeric G protein γ subunit (*GS3/TT2/AT1*) has been shown to regulate grain yield, as well as tolerance to heat and alkaline stress^{1,24,35}. However, the relationship between *AT1* and GA remains unclear and warrants further investigation.

Soil alkalinization is a global issue that severely threatens crop production. The incidence of sodic soils will continue to increase in the future due to global climate change, which will further reduce the global supply of arable land. Therefore, the use of sodic soils for crop production has a great potential to meet the increasing food demands of the human population in the future. Environmental stress has been reported to reduce the GA concentration in plants³¹. Our results showed that exogenous GA₃ supplementation (0.1 μM) markedly enhanced stress tolerance and reduced grain yield loss (Figs. 3a–c, 5j–m, Extended Data Fig. 4a–c and Supplementary Table 10). Thus, our findings provide a new strategy that allows GRVs to be grown on a broad range of alkaline soils with minimal yield loss by simply spraying the foliage with very low levels of the reagent ‘920’ (active ingredient GA₃), which has been widely used for hybrid rice seed production³⁶.

The Green Revolution boosted grain yields in cereal crops by benefiting from the semidwarf phenotypes of GRVs. This phenotype is caused by natural variations in the *ATT1/SD1* alleles, resulting in impaired enzymatic activity or decreased protein levels of the GA20-oxidase *ATT1/SD1*, leading to a differential reduction of GA concentrations in GRVs^{3,4,7,8}. *ATT1/SD1* alleles have been adopted by breeders to develop high-yielding GRVs that are cultivated on arable land worldwide^{37–39}. In this study, we found that the activity of *ATT1/SD1* was more potent than that of *ATT2*, and that genetic manipulation of *ATT1/SD1* could cause notable fluctuations in endogenous GA concentrations (Fig. 2b). Of note, overexpression of *ATT2* in ZH11, a GRV, only slightly increased the GA concentration from a medium level to an optimal medium level, and allowed further enhancement of grain yield and alkali–thermal tolerance in ZH11 (Figs. 1l, 2b and 5d–f,n–p). Thus, *ATT2* is a hitherto overlooked elite allele that could be used for genetic engineering to precisely control endogenous GA concentrations in Green Revolution rice at optimal moderate levels, allowing further improvement in grain yield and alkali–thermal tolerance of GRVs. Therefore, *ATT2* may have great potential to allow plant breeders to address food insecurity caused by the combination of population growth, decreases in

arable land and a rapidly changing climate, and this gene could be an ideal candidate for a future Green Revolution to ensure agricultural sustainability.

Online content

Any methods, additional references, Nature Portfolio reporting summaries, source data, extended data, supplementary information, acknowledgements, peer review information; details of author contributions and competing interests; and statements of data and code availability are available at <https://doi.org/10.1038/s41586-024-08486-7>.

- Zhang, H. et al. A Gy protein regulates alkaline sensitivity in crops. *Science* **379**, eade8416 (2023).
- Zhang, H. et al. A genetic module at one locus in rice protects chloroplasts to enhance thermotolerance. *Science* **376**, 1293–1300 (2022).
- Wu, K. et al. Enhanced sustainable Green Revolution yield via nitrogen-responsive chromatin modulation in rice. *Science* **367**, eaaz2046 (2020).
- Li, S. et al. Modulating plant growth-metabolism coordination for sustainable agriculture. *Nature* **560**, 595–600 (2018).
- Khush, G. S. Green revolution: preparing for the 21st century. *Genome* **42**, 646–655 (1999).
- Hedden, P. The genes of the Green Revolution. *Trends Genet.* **19**, 5–9 (2003).
- Evenson, R. E. & Gollin, D. Assessing the impact of the Green Revolution, 1960 to 2000. *Science* **300**, 758–762 (2003).
- Pingali, P. L. Green revolution: impacts, limits, and the path ahead. *Proc. Natl Acad. Sci. USA* **109**, 12302–12308 (2012).
- Sasaki, A., Ashikari, M., Ueguchi-Tanaka, M., Itoh, H. & Matsuoka, M. A mutant gibberellin-synthesis gene in rice. *Nature* **416**, 701–702 (2002).
- Xue, H., Gao, X., He, P. & Xiao, G. Origin, evolution, and molecular function of DELLA proteins in plants. *Crop J.* **23**, 137–154 (2021).
- Ueguchi-Tanaka, M. et al. *GIBBERELLIN INSENSITIVE DWARF1* encodes a soluble receptor for gibberellin. *Nature* **437**, 693–698 (2005).
- Daviere, J. M. & Achard, P. Gibberellin signaling in plants. *Development* **140**, 1147–1151 (2013).
- Wu, Y. et al. The QTL *GNP1* encodes GA20ox1, which increases grain number and yield by increasing cytokinin activity in rice panicle meristems. *PLoS Genet.* **12**, e1006386 (2016).
- Su, S. et al. Gibberellins orchestrate panicle architecture mediated by DELLA-KNOX signalling in rice. *Plant Biotechnol. J.* **19**, 2304–2318 (2021).
- Stamm, P. & Kumar, P. P. The phytohormone signal network regulating elongation growth during shade avoidance. *J. Exp. Bot.* **61**, 2889–2903 (2010).
- Tang, J. et al. WRKY53 negatively regulates rice cold tolerance at the booting stage by fine-tuning anther gibberellin levels. *Plant Cell* **34**, 4495–4515 (2022).
- Kuroha, T. et al. Ethylene-gibberellin signaling underlies adaptation of rice to periodic flooding. *Science* **361**, 181–185 (2018).
- Colebrook, E. H., Thomas, S. G., Phillips, A. L. & Hedden, P. The role of gibberellin signalling in plant responses to abiotic stress. *J. Exp. Biol.* **217**, 67–75 (2014).
- Intergovernmental Technical Panel on Soils. *Salt-affected soils are a global issue* (FAO, 2021).
- Adam, D. How far will global population rise? *Nature* **597**, 462–465 (2021).
- Matthews, H. D. & Wynes, S. Current global efforts are insufficient to limit warming to 1.5°C. *Science* **376**, 1404–1409 (2022).
- Zhao, C. et al. Temperature increase reduces global yields of major crops in four independent estimates. *Proc. Natl Acad. Sci. USA* **114**, 9326–9331 (2017).
- Fan, C. H. et al. GS3, a major QTL for grain length and weight and minor QTL for grain width and thickness in rice, encodes a putative transmembrane protein. *Theor. Appl. Genet.* **112**, 1164–1171 (2006).
- Mao, H. L. et al. Linking differential domain functions of the GS3 protein to natural variation of grain size in rice. *Proc. Natl Acad. Sci. USA* **107**, 19579–19584 (2010).
- Li, J. et al. An endoplasmic reticulum-associated degradation-related E2-E3 enzyme pair controls grain size and weight through the brassinosteroid signaling pathway in rice. *Plant Cell* **35**, 1076–1091 (2023).
- Yamaguchi, S. Gibberellin metabolism and its regulation. *Ann. Rev. Plant Biol.* **59**, 225–251 (2008).
- Hedden, P. Gibberellin metabolism and its regulation. *J. Plant Growth Regul.* **20**, 317–318 (2001).
- Shohat, H. et al. Inhibition of gibberellin accumulation by water deficiency promotes fast and long-term ‘drought avoidance’ responses in tomato. *New Phytol.* **232**, 1985–1998 (2021).
- Rizza, A., Walia, A., Lanquar, V., Frommer, W. B. & Jones, A. M. In vivo gibberellin gradients visualized in rapidly elongating tissues. *Nat. Plants* **3**, 803–813 (2017).
- Achard, P., Renou, J. P., Berthome, R., Harberd, N. P. & Genschik, P. Plant DELLA proteins restrain growth and promote survival of adversity by reducing the levels of reactive oxygen species. *Curr. Biol.* **18**, 656–660 (2008).
- Achard, P. et al. Integration of plant responses to environmentally activated phytohormonal signals. *Science* **311**, 91–94 (2006).
- Mittler, R., Vanderauwera, S., Gollery, M. & Van Breusegem, F. Reactive oxygen gene network of plants. *Trends Plant Sci.* **9**, 490–498 (2004).
- Takahashi, M., Nakanishi, H., Kawasaki, S., Nishizawa, N. K. & Mori, S. Enhanced tolerance of rice to low iron availability in alkaline soils using barley nicotianamine aminotransferase genes. *Nat. Biotechnol.* **19**, 466–469 (2001).

34. Wu, N. et al. A MITE variation-associated heat-inducible isoform of a heat-shock factor confers heat tolerance through regulation of JASMONATE ZIM-DOMAIN genes in rice. *New Phytol.* **234**, 1315–1331 (2022).
35. Kan, Y. et al. *TT2* controls rice thermotolerance through SCT1-dependent alteration of wax biosynthesis. *Nat. Plants* **8**, 53–67 (2022).
36. Chen, H., Jiang, S., Zheng, J. & Lin, Y. J. Improving panicle exertion of rice cytoplasmic male sterile line by combination of artificial microRNA and artificial target mimic. *Plant Biotechnol. J.* **11**, 336–343 (2013).
37. Asano, K. et al. Artificial selection for a Green Revolution gene during *japonica* rice domestication. *Proc. Natl Acad. Sci. USA* **108**, 11034–11039 (2011).
38. Gao, S. P. & Chu, C. C. Gibberellin metabolism and signaling: targets for improving agronomic performance of crops. *Plant Cell Physiol.* **61**, 1902–1911 (2020).
39. Sha, H. J. et al. Elite *sd1* alleles in *japonica* rice and their breeding applications in northeast China. *Crop J.* **10**, 224–233 (2022).

Publisher's note Springer Nature remains neutral with regard to jurisdictional claims in published maps and institutional affiliations.

Springer Nature or its licensor (e.g. a society or other partner) holds exclusive rights to this article under a publishing agreement with the author(s) or other rightsholder(s); author self-archiving of the accepted manuscript version of this article is solely governed by the terms of such publishing agreement and applicable law.

© The Author(s), under exclusive licence to Springer Nature Limited 2025

Article

Methods

Plant materials and growth conditions

We constructed a set of CSSLs (chromosomal segment substitution lines, designated BAS) in which the African wild rice species *O. barthii* (BART) was the donor parent and the *indica* variety 'Longtepu' (LTP) was the recurrent parent, and used them to clone and identify QTL for alkali and heat stress. Two CSSLs containing *ATT1* (named BA5) and *ATT2* (named BA17) that are sensitive to alkali-thermal stresses compared to LTP were selected and backcrossed several times to LTP. To fine map *ATT1* and *ATT2*, we selected plants that were heterozygous for *ATT1* and *ATT2* but were homozygous for almost all other regions from LTP and used them to develop the two segregating BC₅F₂ populations by marker-assisted selection. We constructed NILs of *ATT1* (NIL-*ATT1*^{BART}) and *ATT2* (NIL-*ATT2*^{BART}) that carry very small *O. barthii* chromosomal regions containing the *ATT1* and *ATT2* loci in the LTP genetic background. We also constructed the isogenic controls NIL-*ATT1*^{LTP} and NIL-*ATT2*^{LTP}. The mutants 9311-ngr5, NJ6-att1, NJ6-gid1 and 9311-lc2 and the transgenic overexpression lines p35S::NGR5-HA, p35S::LC2-HA are described in a previous study³. The knockout mutants *att1* and *att1/att2* and the overexpression transgenic line p35S::*ATT1* in the Nipponbare background were described elsewhere¹⁴. The overexpression transgenic line p35S::*ATT2* in the ZH11 background was made as described elsewhere¹³. The CRISPR-Cas9 system was used to create the *att2* mutant in the ZH11 background, following the method previously described⁴⁰. The knockout of *ATT1* in the NIL-*ATT1*^{BART} background (*att1*/NIL-*ATT1*^{BART}), *ATT2* in the NIL-*ATT2*^{LTP} background (*att2*/NIL-*ATT2*^{LTP}) and *ATT2* in the NJ6 (*att2*^{NJ6}) or *att1*^{NJ6} backgrounds (*att1*^{NJ6}/*att2*^{NJ6}) was also achieved using this gene-editing approach as outlined elsewhere^{41,42}. Furthermore, the genomic DNA of *ATT1*^{BART} or *ATT2*^{LTP} was introduced into the NIL-*ATT1*^{LTP} (g*ATT1*^{BART}/NIL-*ATT1*^{LTP}) or NIL-*ATT2*^{BART} (g*ATT2*^{LTP}/NIL-*ATT2*^{BART}) backgrounds, respectively. Transgenic plant materials were produced through *Agrobacterium tumefaciens*-mediated transformation^{43,44}. The primers used in this study are listed in Supplemental Table 11.

The rice lines and populations used in this study were grown in natural rice fields at Shanghai (from May to October) and Hainan (from November to April of the following year). The transgenic plants were grown in a greenhouse with a 12 h of light (25 °C)/12 h of dark (25 °C) photoperiod. Plants grown in the field were transferred to pots for photographing.

Plant culture and identification of alkali-thermal tolerant plants

Rice seedlings were cultivated in Yoshida solution (pH 5.8) at 28 °C, 60% relative humidity under a 14 h light/10 h dark photoperiod and 12-day-old seedlings were used in the alkali and high temperature treatments. For alkali stress, the rice seedlings were transferred to a hydroponic culture solution containing 65 mM NaHCO₃ and grown for 7–14 days. For heat stress, 12-day-old seedlings grown in Yoshida solution were transferred to a chamber (Climacell EVO 707). For the heat treatment, seedlings were exposed to a temperature of 42 °C with 90% relative humidity for 20–28 h. To determine the survival rate after alkali and heat treatment, seedlings were allowed to recover under normal growth conditions in a timely manner to prevent over-treatment. After 7 days of recovery, the death of young leaves was used as an indicator of seedling death, as the death of young leaves ultimately leads to the demise of the entire seedling. The survival rate was then calculated as the ratio of the number of surviving seedlings to the total number of seedlings.

Map-based cloning of *ATT1* and *ATT2*

We used the two BC₅F₂ populations carrying the *ATT1* and *ATT2* regions that were derived from a cross between the African wild rice species *O. barthii* and the *indica* variety 'Longtepu' (LTP). To fine map the *ATT1* and *ATT2* sites, homozygous recombinant plants were selected for

identification of their heat and alkali tolerance phenotypes, respectively. A total of 30,900 individuals were selected for genetic analysis. Using 21 new INDEL markers, *ATT1* was located to a region of 174.75 kb on chromosome 1 and *ATT2* was located to a region of 47.25 kb on chromosome 3. At the same time, the 174.75 and 47.25-kb regions in BC₅F₂-generation plants were used to construct the *ATT1* and *ATT2* NILs. The candidate *ATT1* and *ATT2* genes in the 'Longtepu' and *O. barthii* genomes were sequenced and analysed, and the sequences were compared by MegAlign Pro (DNASTAR v.11.0). The names and DNA sequences of the primers used for map-based cloning and genotyping assays are given in Supplementary Table 11.

RNA extraction and RT-qPCR

Total RNA was extracted from rice tissues using the SteadyPure Universal RNA Extraction Kit II (AG). RNA samples (100–1,000 ng) from each sample were reverse-transcribed into first-strand complementary DNA using the HiScript III RT SuperMix for qPCR (+gDNA wiper) according to the manufacturer's instructions for subsequent RT-qPCR. The ChamQ SYBR qPCR Master Mix (without reference dye) was used to perform RT-qPCR analysis on a QIAquant 96 2plex Real-Time PCR System. Analysis of each sample was performed with at least three biological replicates, and gene expression was normalized against the rice *OsActin* gene. The names and sequences of the primers used for gene amplification are given in Supplementary Table 11.

Quantification of the levels of GAs

For rice seedlings plants: seedlings were grown for 12 days under normal conditions, and 24 seedlings were harvested, flash frozen in liquid nitrogen and ground to a powder. The contents of endogenous GAs (GA₁, GA₄, GA₉, GA₁₂, GA₁₉, GA₂₀, GA₂₄ and GA₅₃) in the seedlings were measured by the Wuhan Greensword Creation Technology Company. For rice plants at the booting stage: the plants were initially grown under normal conditions until they reached the booting stage. They were then subjected to an alkaline treatment with 150 mM sodium bicarbonate for either 7 or 14 days, followed by heat treatments at 45 °C, with relative humidity greater than 90% for 2 or 4 days. After these treatments, stems (topmost internodes), leaves (penultimate leaves) and 5–10-cm panicles were harvested and immediately frozen in liquid nitrogen. The levels of endogenous GAs (GA₁, GA₄) in the stems, leaves and panicles were subsequently measured by the CAS Center for Excellence in Molecular Plant Sciences-Core Facility Center.

GA and PAC treatments

Six-day-old seedlings grown under the normal conditions were treated with GA (GA₃) or PAC for 6 days. Following the treatments, the now 12-day-old seedlings were used in the heat or alkali treatments.

Plant protein extraction and western blot analysis

Twelve-day-old rice seedling tissues were harvested, frozen in liquid nitrogen and ground to a powder. The powdered samples were then suspended in precooled extraction buffer (NP-40 Lysis buffer, PS0010), and the lysates were centrifuged at 12,000 rpm for 5 min at 4 °C to remove the insoluble debris. Next, the protein-containing supernatants were collected, mixed with SDS loading buffer and then boiled for 10 min. The proteins in the sample extracts were separated by sodium dodecyl sulfate denaturing polyacrylamide gel electrophoresis (SDS-PAGE). The endogenous SLR1 protein levels in the NIL-*ATT1*^{LTP} and NIL-*ATT1*^{BART} plants, as well as in the NIL-*ATT2*^{LTP} and NIL-*ATT2*^{BART} plants, were visualized by immunoblot analysis using the rabbit polyclonal anti-SLR1 antibody (Abmart, P46081R1, 1:2,000 dilution). The loading control was blotted using the anti-ACTIN antibody (Abmart, M20009, 1:2,000 dilution). The secondary antibodies used were goat-Anti-Mouse IgG (H+L) (Proteintech, SA00001-1, 1:10,000

dilution) and goat-Anti-Rabbit IgG (H+L) (Proteintech, SA00001-2, 1:10,000 dilution).

Quantitative determination of ROS

Determination of POX activity and ROS levels was performed using leaves from 12-day-old rice seedlings with or without heat and alkali treatment. POX and ROS were extracted in 20 mM phosphate buffer (pH 6.5, precooled to 4 °C) and the extracts were centrifuged at 12,000 rpm, 4 °C for 10 min. Next, the supernatant was analysed to determine POX activities and H₂O₂ contents using the Amplex Red Hydrogen Peroxide/Peroxidase Assay Kit as directed by the manufacturer (Molecular Probes).

DAB and NBT staining

The 3,3'-diaminobenzidine (DAB) and nitro-blue tetrazolium (NBT) staining was conducted using leaves from 12-day-old seedlings with or without alkali and heat treatments. The samples were treated with NBT (1 mg ml⁻¹ NBT in 10 mM phosphate buffer, pH 7.8) or DAB solutions (1 mg ml⁻¹ DAB-HCl, pH 3.8). After staining, the leaves were boiled in 95% ethanol for 2–4 h to eliminate chlorophyll before imaging.

GUS staining

Transgenic *ProATT1::GUS* and *ProATT2::GUS* plants in ZH11 background were grown to the booting stage under normal conditions. They were then subjected to either a 1- or 3-day heat treatment (150 mM sodium bicarbonate) or 1 or 3 days of heat treatment (45 °C, RH > 90%). Following treatment, root, stems, leaves and panicles were collected. The tissues were stained using a GUS staining kit (Coolaber, SL7160). Samples were immersed in GUS staining buffer, vacuum infiltrated for 30 min and incubated at 37 °C for 4–10 h. Chlorophyll was removed using 75% ethanol until complete decolorization, after which the samples were photographed.

Protein expression in *E. coli*

The gene coding sequences were cloned onto the pMAL-c5x vector (New England Biolabs), and the constructs were transformed into the *Escherichia coli* BL21 (DE3) pLysS. The strains were cultured in Luria-Bertani medium containing 50 mg l⁻¹ sodium carbenzyl penicillin at 37 °C to an optical density at 600 nm (OD₆₀₀) of 0.4–0.6. Expression of the NGR5, ATT1 and ATT2 proteins was induced by adding 0.5 mM isopropyl-β-D-thiogalactoside (IPTG) (YEASEN) and incubated at 16 °C for 20 h. The cells were collected by centrifugation (4,000g for 5 min) at 4 °C and resuspended in 1 ml of extraction buffer (100 mM NaCl, 20 mM Tris-HCl, pH 8.0). Appropriate amounts of protease inhibitor-cComplete Tablets EDTA-free, EASYpack (Roche), phenylmethylsulfonyl fluoride (PMSF) (YEASEN) and DDT were added to the cell suspensions. The bacterial cells were then lysed using a protein press and centrifuged at 10,000 rpm at 4 °C for 10 min to obtain the supernatant, which was used as the crude protein extract. Recombinant proteins were purified using the ÄKTA purification platform (cytiva) with MBPTrap HP-5mL (cytiva) following the manufacturer's instructions. Some purified protein solution samples were added to concentrated SDS loading buffer for denaturation. After boiling for 10 min, the samples were separated by SDS-PAGE and the protein expression was measured by Coomassie Brilliant Blue staining. The relevant primer sequences are given in Supplementary Table 11.

DNA and RNA-seq

Total RNA from all samples was extracted from rice tissues using the SteadyPure Universal RNA Extraction Kit II, and the RNA samples were treated with the DNase enzyme provided in the kit. RNA samples (for RNA-seq) and leaf (for DNA sequencing) were outsourced to company for quality inspection, library building, nucleotide sequencing and data analysis.

Enzyme activities of ATT1 and ATT2

Twelve-day-old seedlings of the *att1att2* mutant (Nipponbare background) were harvested and ground into fine powders. Precisely 2.0 g of the powdered sample was weighed and mixed with 13 ml of acetonitrile in a grinding tube. The mixture was vortexed, placed in an ultrasonic water bath with ice for 3 min and then extracted overnight at 4 °C with shaking at 1,000 rpm. For centrifugation and supernatant transfer, the sample was centrifuged at 15,000 rpm for 20 min at 4 °C, and then the supernatant was transferred to a new tube and evaporate to dryness under nitrogen gas. For precipitate extraction with ethyl acetate, 6 ml of ethyl acetate was added to the precipitate left in the original tube, mixed thoroughly and centrifuged again at 15,000 rpm for 20 min at 4 °C. The supernatant was transferred to a new tube and evaporated to dryness under nitrogen gas. For resuspension in reaction buffer, 5 ml of reaction buffer was added to the remaining precipitate. The reaction buffer consisted of 20 mM Tris (pH 8.0), 0.5 mM DTT, 0.1 mM PMSF and 1× protease inhibitor-cComplete Tablets (EDTA-free). The solution was mixed well to resuspend the precipitate. For the enzyme reaction setup, a 750 µl aliquot of the reaction buffer containing the total GAs was distributed into separate tubes, after which 50 µl of recombinant ATT1-MBP, ATT2-MBP, MBP (control) (recombinant protein were diluted to the same concentration) or water (control) were added to each tube. We ensured the protein concentration was the same across all samples, and incubated the reaction mixture for 20 min at 25 °C. To stop the enzyme reaction, 800 µl of acetonitrile were added to each reaction mixture to stop the enzyme activity. For product measurement, the samples were sent to Wuhan Greensword Creation Technology Co. Ltd for quantification of GA₉ and GA₂₀, the products of GA20-oxidase activity.

EMSA

EMSA were performed as previously described⁴⁵. Recombinant MBP-NGR5 protein was produced in *E. coli* as described in the sections 'Protein expression in *E. coli*' and 'Plant protein extraction and western blot analysis' above. DNA probes (the T3 fragment for the *OsNAAT1* gene, the F4 fragment for the *OsHsfA2d* gene) were amplified and labelled with CYS. DNA gel-shift assays were performed using the chemiluminescence EMSA kit (Baiyun, GS005) and detection and image capture were performed using the UVP Chemstudio touch (Analytik Jena AG). The relevant probe sequences are shown in Supplementary Table 11.

ChIP-PCR assay

The ChIP-PCR assay was conducted according to the ChIP Assay method for rice in ref. 46. Three grams of 12-day-old rice seedlings were rapidly fixed by infiltration with 1% (v/v) formaldehyde under vacuum at 25 °C for 15 min, after which they were ground to a powder in liquid nitrogen. The cell nuclei were separated and lysed, and protein-DNA complexes were immunoprecipitated with the rabbit polyclonal anti-H3K27me3 antibody (Abclonal, A2363), the anti-H3 antibody (Abclonal, A2348) and the anti-HA antibody (Proteintech, 51064-2-AP), with a dilution of 1:200. The co-immunoprecipitated DNA was retrieved and then analysed by RT-qPCR. Each result is based on at least three biological replicates, and each biological replicate consisted of at least four technical replicates. The relevant primer sequences are given in Supplementary Table 11.

Evaluation of yield performance under normal, alkali and heat-stress conditions

We investigated the grain yield traits of *ATT1* and *ATT2* in different backgrounds under heat treatment, alkali treatment and normal growing conditions from 2021 to 2024. The field trials were conducted at the Experimental Farm in Shanghai and Hainan (Sanya), China. To evaluate the alkali tolerance of the *ATT1* and *ATT2* NILs and overexpression-*ATT2*

Article

transgenic rice plants at the adult stage, plants were cultivated in alkaline and normal soils in the fields, respectively, throughout the entire growth period. 'Longtepu' and 'Songxianggenda' with or without GA₃ treatment in alkaline and normal soils in a greenhouse. The pH, oxidation reduction potential and salt content of the test soils were measured during the treatment. For the alkaline soil, the pH value was maintained at roughly 9.0. To evaluate the heat tolerance, sunlight-heated plastic greenhouses were set up during the grain-filling period and were used until the seeds matured in the experimental fields. At maturity, we measured plant height, tiller number, panicle length (main panicle), grain numbers per panicle (main panicle), setting percentage (main panicle), grain length, grain width, 1,000-grain weight and grain yield per plant or per plot.

Statistical analysis

In this study, all analyses were performed using Microsoft Excel v.2016 and GraphPad Prism v.8.0 software, and the values are shown as mean \pm s.d. The numbers (*n*) of samples or biological replicates are described in detail in the figure legends. Significant differences between two groups were determined with a two-sided Student's *t*-test; differences between three or more groups were determined using two-way analysis of variance (ANOVA) with a least-significant difference (LSD) test.

Accession numbers

Accession numbers are as follows: *ATT1* (GA20-oxidase 2/*SD1*, LOC_Os01g66100); *ATT2* (GA20-oxidase 1/*GNP1*, LOC_Os03g63970); *GID1*, LOC_Os05g33730; *SLR1*, LOC_Os03g49990; *OsGA2ox1*, LOC_Os05g06670; *OsGA2ox2*, LOC_Os01g22910; *OsGA2ox3*, LOC_Os01g55240; *OsGA2ox4*, LOC_Os05g43880; *OsGA2ox5*, LOC_Os07g01340; *OsGA2ox6*, LOC_Os04g44150; *OsGA2ox7*, LOC_Os01g11150; *OsGA2ox8*, LOC_Os05g48700; *OsGA2ox9*, LOC_Os02g41954; *OsGA2ox10*, LOC_Os05g11810; *EUI1*, LOC_Os05g40384; *OsAPXa*, LOC_Os03g17690; *OsAPXb*, LOC_Os07g49400; *ALM1*, LOC_Os06g05110; *MnSOD1*, LOC_Os05g25850; *OscATA*, LOC_Os02g02400; *OsCATB*, LOC_Os06g51150; *OsCATC*, LOC_Os03g03910; *NGR5*, LOC_Os05g32270; *LC2*, LOC_Os02g05840; *OsNAAT1*, LOC_Os02g20360 and *OsHsfA2d*, LOC_Os03g06630.

Reporting summary

Further information on research design is available in the Nature Portfolio Reporting Summary linked to this article.

Data availability

All data are available within this Article and its Supplementary Information. Original gel blots are shown in Supplementary Information Fig. 1. The candidate genes in *ATT1* and *ATT2* chromosomal region and accession numbers were obtained from the MSU (Michigan State University Rice Genome Annotation Project) database (<http://rice.plantbiology.msu.edu/>). The DNA next-generation genome sequencing data

generated in this study have been deposited at the National Genomics Data Center under accession number (ID CRA019914). The RNA-seq data generated in this study have been deposited at the National Genomics Data Center under accession number ID CRA019913. Source data are provided with this paper.

40. Ma, X. L. et al. A robust CRISPR/Cas9 system for convenient, high-efficiency multiplex genome editing in monocot and dicot plants. *Mol. Plant* **8**, 1274–1284 (2015).
41. Chen, K. et al. A FLASH pipeline for arrayed CRISPR library construction and the gene function discovery of rice receptor-like kinases. *Mol. Plant* **15**, 243–257 (2022).
42. Xie, K., Minkenberg, B. & Yang, Y. Boosting CRISPR/Cas9 multiplex editing capability with the endogenous tRNA-processing system. *Proc. Natl Acad. Sci. USA* **112**, 3570–3575 (2015).
43. Chen, Q. H., Chen, T. Y., Lin, Y. J. & Chen, H. Agrobacterium-mediated genetic transformation of Japonica rice. *Bio-101* <https://doi.org/10.21769/BioProtoc.1010174> (2018).
44. Liu, Y., Ling, F., Lin, Y. J. & Chen, H. Agrobacterium-mediated transformation of Indica rice. *Bio-101* <https://doi.org/10.21769/BioProtoc.1010175> (2018).
45. Chen, K. et al. Translational regulation of plant response to high temperature by a dual-function tRNA(His) guanylyltransferase in rice. *Mol. Plant* **12**, 1123–1142 (2019).
46. Weng, X. Y., Zhou, S. L., Chong, W. & Ouyang, Y. D. ChIP assay in rice. *Bio-101* <https://doi.org/10.21769/BioProtoc.1010135> (2018).

Acknowledgements We thank Y. Liu (South China Agriculture University) and K. Xie (Huazhong Agriculture University) for donation of CRISPR-Cas9 plasmids; X. Fu (Institute of Genetics and Developmental Biology, Chinese Academy of Sciences) and D. Zhang (Shanghai Jiao Tong University) for providing seeds of some rice genetic materials; H. Liu and C. Shi (Centre for Excellence in Molecular Plant Sciences, CAS) for help with ChIP-PCR assay; Y. Gao and W. Hu (Centre for Excellence in Molecular Plant Sciences, CAS) for technical assistance on quantification of the levels of GAs. This work was supported by the grants from Biological Breeding-National Science and Technology Major Project (grant no. 2023ZD0407103), National Natural Science Foundation of China (grant no. 32388201), Shanghai Jiao Tong University 2030 Initiative, the Shanghai Collaborative Innovation Center of Agri-Seeds (ZXWH2150201), National Key Research and Development Program of China (grant no. 2022YFD1200102, 2024YFF1000402), Shanghai Pujiang Program (grant no. 22PJ1406500), Chinese Academy of Sciences (grant no. 159231KYSB20200008), Laboratory of Lingnan Modern Agriculture Project (grant no. NT2021002) and CAS-Croucher Funding Scheme for Joint Laboratories.

Author contributions H.-X.L. and Y.L. conceived and supervised the project. H.-X.L., Y.L. and S.-Q.G. designed the experiments. S.-Q.G. and Y.-X.C. performed most of the experiments, including the QTL mapping, molecular cloning, the transformation work, alkali-thermal tolerant assays, western blots, RNA extraction, RT-qPCR, quantification of the levels of GAs, GA and PAC treatments, plant protein extraction and western blot analysis, quantitative determination of ROS, DAB and NBT staining, GUS staining, enzyme activities and evaluation of yield performance under normal, alkali and heat-stress conditions. Y.-L.J. and C.-Y.P. performed protein expression, EMSAs and ChIP-PCR assay. J.-X.S. performed management of rice materials in paddy fields and construction of chromosomal segment substitution lines. W.-W.Y. and N.-Q.D. performed storage of rice material seeds and daily experiment management. Y.K., Y.-B.Y., H.-Y.Z., H.-X.Y., Z.-Q.L., J.-J.L., B.L., X.-R.M., Y.-J.C., L.G., J.G., J.-F.Z. and K.-Y.Y. contributed to seed harvest and investigation of some agronomic traits in the field. S.-Q.G. analysed data. Y.L., S.-Q.G. and H.-X.L. wrote the manuscript.

Competing interests The authors declare no competing interests.

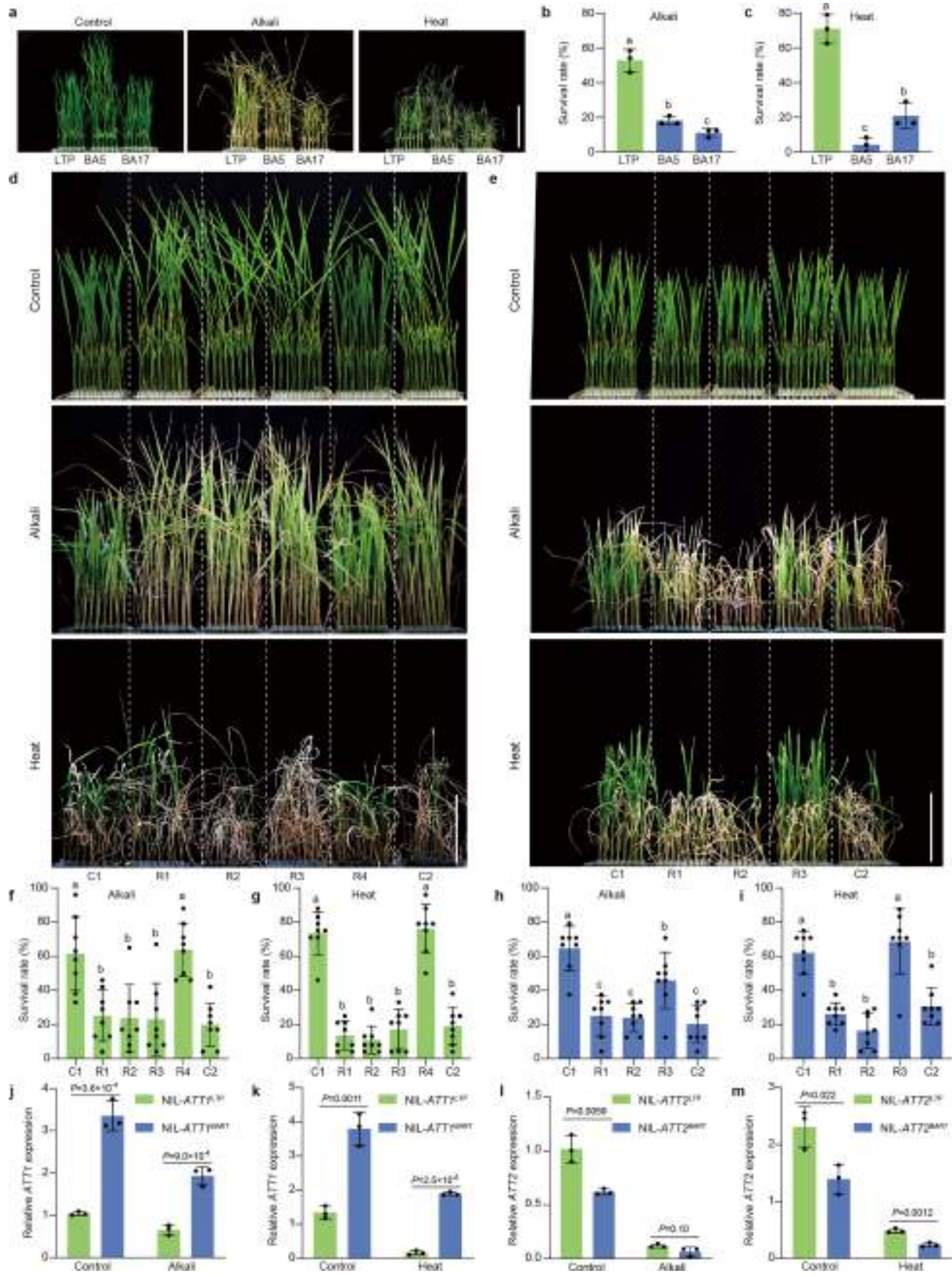
Additional information

Supplementary information The online version contains supplementary material available at <https://doi.org/10.1038/s41586-024-08486-7>.

Correspondence and requests for materials should be addressed to Hong-Xuan Lin or Youshun Lin.

Peer review information *Nature* thanks Patrick Achard, Xiangdong Fu and the other, anonymous, reviewer(s) for their contribution to the peer review of this work. Peer reviewer reports are available.

Reprints and permissions information is available at <http://www.nature.com/reprints>.

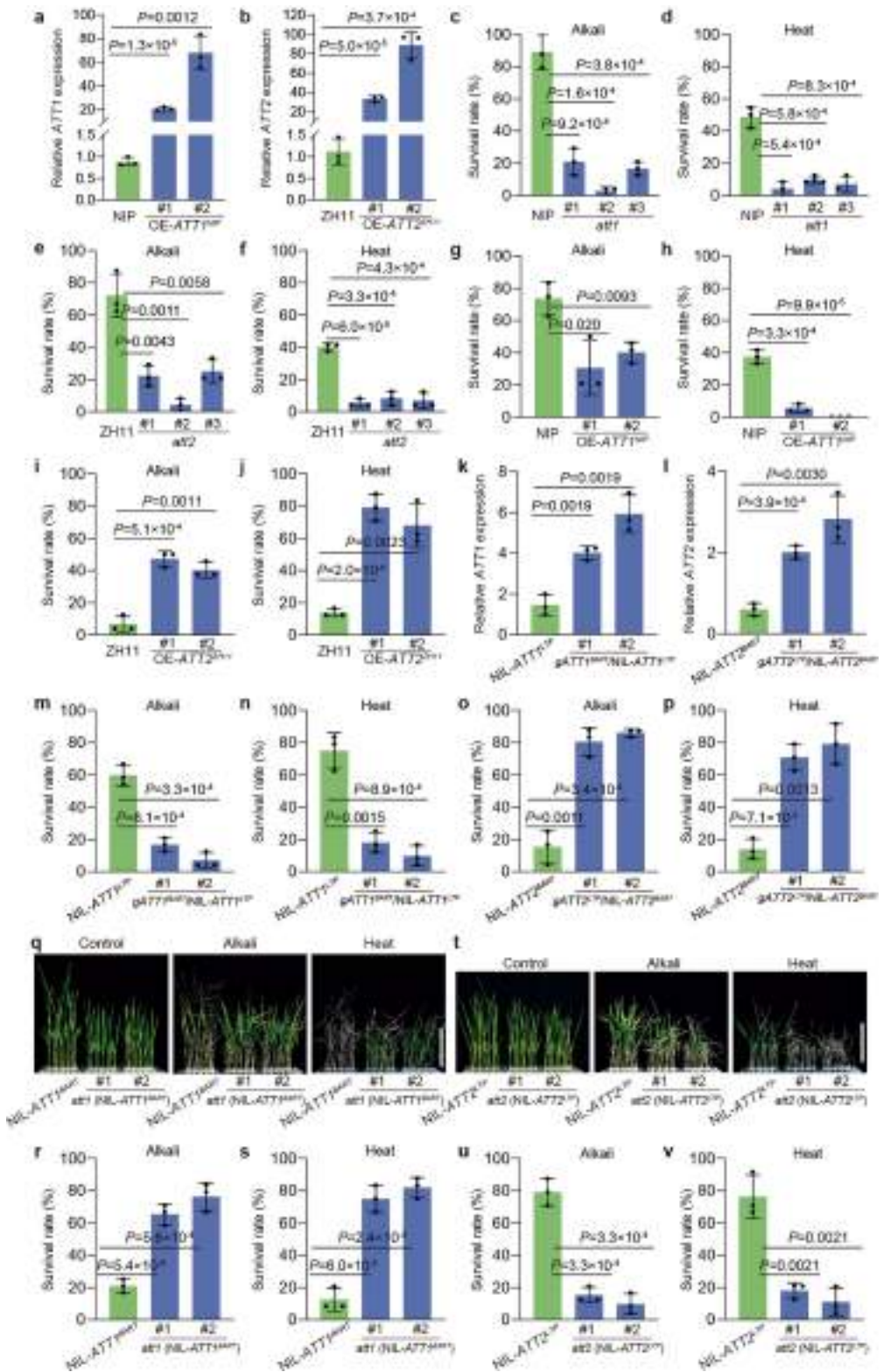


Extended Data Fig. 1 | See next page for caption.

Article

Extended Data Fig. 1 | Identification and fine mapping of *ATT1* and *ATT2* for alkali-thermal tolerance in rice. **a-c**, Phenotypic responses to alkali and high temperature treatments of the BA CSSLs (**a**) and the survival rates under stress (**b,c**) ($n = 3$, biologically independent samples, each sample consisted of 24 seedlings). **d,e**, Phenotypic responses to alkali and high temperature treatments of recombinant lines in the regions of *ATT1* (**d**) and *ATT2* (**e**). Scale bars = 10 cm. **f-i**, Survival rates of the recombinant lines C1 and C2 and R1-R4 (or R1-R3) in the alkali (**f,h**) and heat (**g,i**) treatments, respectively ($n = 8$, biologically independent samples, each sample consisted of 24 seedlings). **a-i**, Alkali treatment, 65 mM sodium bicarbonate for 14 days; Heat treatment,

42 °C and RH > 90% for 28 h; 12-day-old plants were subjected to stress treatments and then recovered for 7 days; scale bars = 10 cm. **j-m**, Relative expression of *ATT1* (**j,k**) and *ATT2* (**l,m**) in NIL-*ATT1^{LTP}* and NIL-*ATT1^{BART}*, and NIL-*ATT2^{LTP}* and NIL-*ATT2^{BART}* with or without alkali treatment (**j,l**) (65 mM sodium bicarbonate, 24 h) and heat treatment (**k,m**) (42 °C, RH > 90%, 3 h) ($n = 3$, biologically independent samples). The values in **b,c,f-i** represent the mean ± s.d.; In **b,c,f-i**, the same lower-case letters indicate no significant difference at $p > 0.05$ as determined by two-way ANOVA with LSD test; In **j-m**, two-tailed Student's *t*-tests were used to determine *P* values.

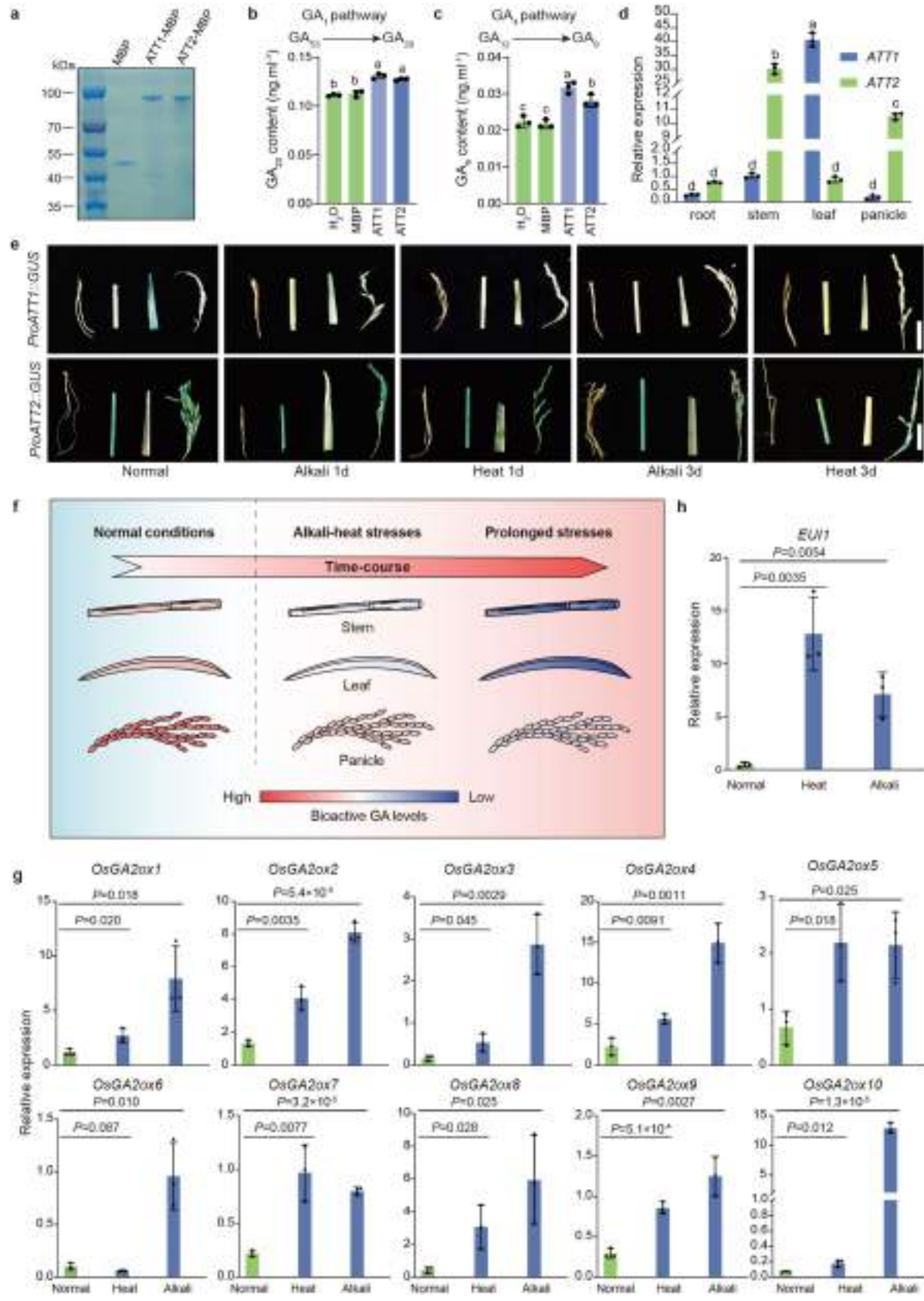


Extended Data Fig. 2 | See next page for caption.

Article

Extended Data Fig. 2 | Transgenic verification of *ATT1* and *ATT2* for alkali-thermal tolerance in rice. **a**, Relative expression of *ATT1* in ‘Nipponbare’ and OE-*ATT1*^{NP} transgenic lines. **b**, Relative expression of *ATT2* in ZH11 and OE-*ATT2*^{ZH11} transgenic lines. **c-f**, Survival rates of ‘Nipponbare’ and *att1* mutant lines (**c,d**), ZH11 and *att2* mutant lines (**e,f**) under alkali and heat treatments. **g-j**, Survival rates of ‘Nipponbare’ and OE-*ATT1*^{NP} transgenic lines (**g,h**), and ZH11 and OE-*ATT2*^{ZH11} transgenic lines (**i,j**) under alkali and heat treatments. **k**, Relative expression of *ATT1* in NIL-*ATT1*^{LTP} and transgenic complementation lines containing the *ATT1* genomic DNA from NIL-*ATT1*^{BART} in NIL-*ATT1*^{LTP} background (*gATT1*^{BART}/NIL-*ATT1*^{LTP}). **l**, Relative expression of *ATT2* in NIL-*ATT2*^{BART} and transgenic complementation lines containing the *ATT2* genomic DNA from NIL-*ATT2*^{LTP} in NIL-*ATT2*^{BART} background (*gATT2*^{LTP}/NIL-*ATT2*^{BART}). **m-p**, Survival

rates of NIL-*ATT1*^{LTP} and two *ATT1* complementation transgenic lines, NIL-*ATT2*^{BART} and two *ATT2* complementation transgenic lines after alkali and heat treatments. **q-v**, Phenotypes (**q,t**) and survival rates (**r,s,u,v**) of NIL-*ATT1*^{BART} and *att1* (NIL-*ATT1*^{BART}) (**r,s**), NIL-*ATT2*^{LTP} and *att2* (NIL-*ATT2*^{LTP}) (**u,v**) after alkali and heat treatments. Alkali treatment [65 mM sodium bicarbonate, 10 days (**c,e,g**), 11 days (**i**), 14 days (**m,o,q,r,t,u**)] and heat treatment [42°C, RH > 90%, 20 h (**d,f,h**), 22 h (**j**), 28 h (**n,p,q,s,t,v**)]; 12-day-old seedlings were subjected to stress treatments and then recovered for 7 days; scale bars = 10 cm. The values in **a-p,r,s,u,v** represent the mean \pm s.d.; $n = 3$, biologically independent samples, each sample consisted of 24 seedlings; In **a-p,r,s,u,v**, two-tailed Student’s *t*-tests were used to determine *P* values.



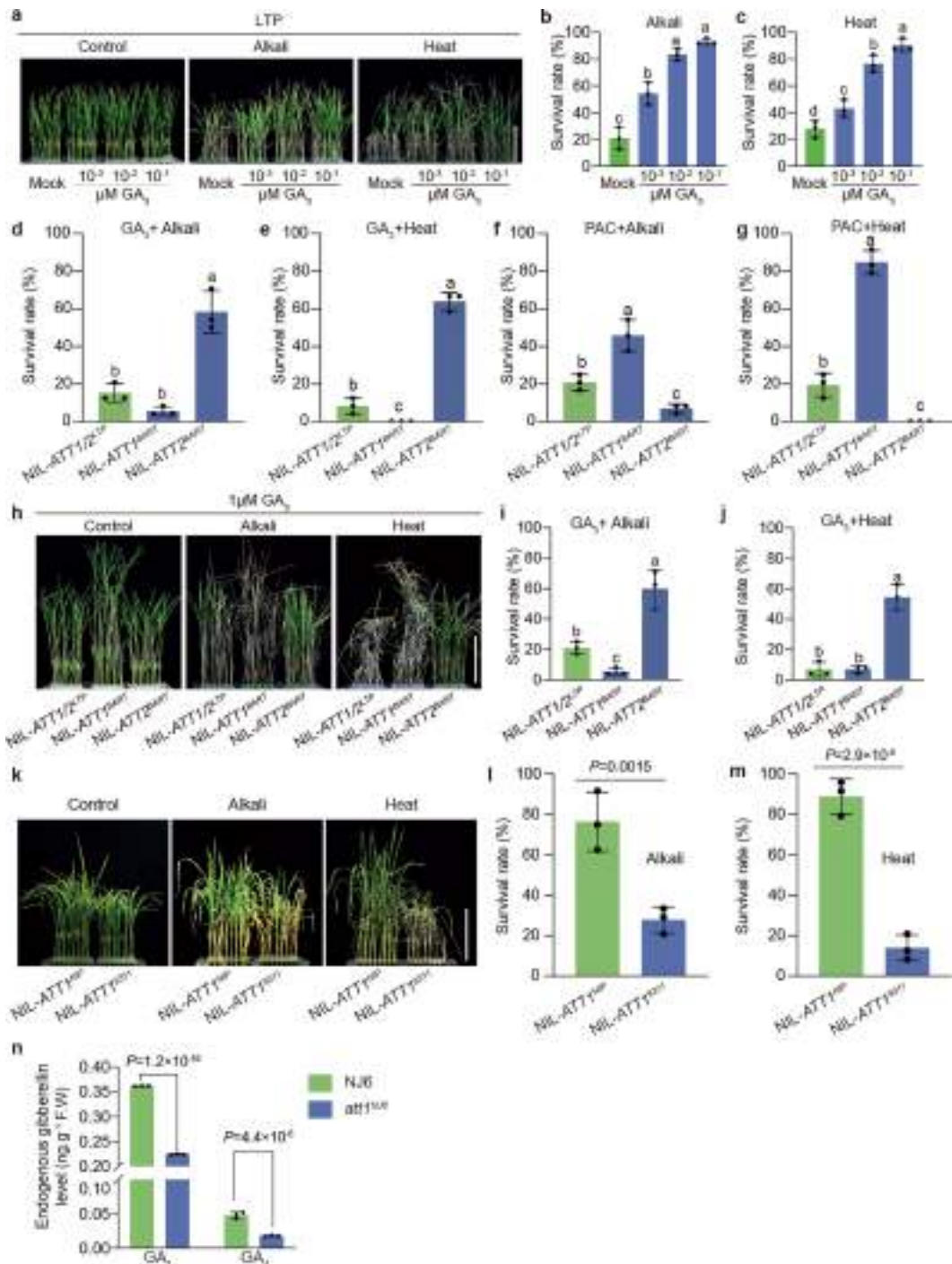
Extended Data Fig. 3 | See next page for caption.

Article

Extended Data Fig. 3 | *ATT1* and *ATT2* modulate gibberellin synthesis.

a, Purification of MBP-*ATT1* and MBP-*ATT2* fusion proteins. Purified MBP (1.5 µg), recombinant *ATT1* proteins (MBP-*ATT1*; 3.0 µg) and recombinant *ATT2* proteins (MBP-*ATT2*; 3.0 µg) were separated using SDS-PAGE gels before Coomassie Brilliant Blue staining. **b,c**, Enzymatic activities of recombinant *ATT1* and *ATT2* proteins involved in GA₁ (**b**) and GA₄ (**c**) synthesis pathways. MBP, refers to maltose-binding protein. **d**, Expression profile of *ATT1* and *ATT2* in roots, stems, leaves and panicles of rice plants at the booting stage. **e**, Expression patterns of *ATT1:GUS* (β -glucuronidase) and *ATT2:GUS* in roots, stems, leaves and panicles of rice plants at the booting stage under normal conditions, alkali (150 mM sodium bicarbonate, 1 d or 3 d) and heat treatments

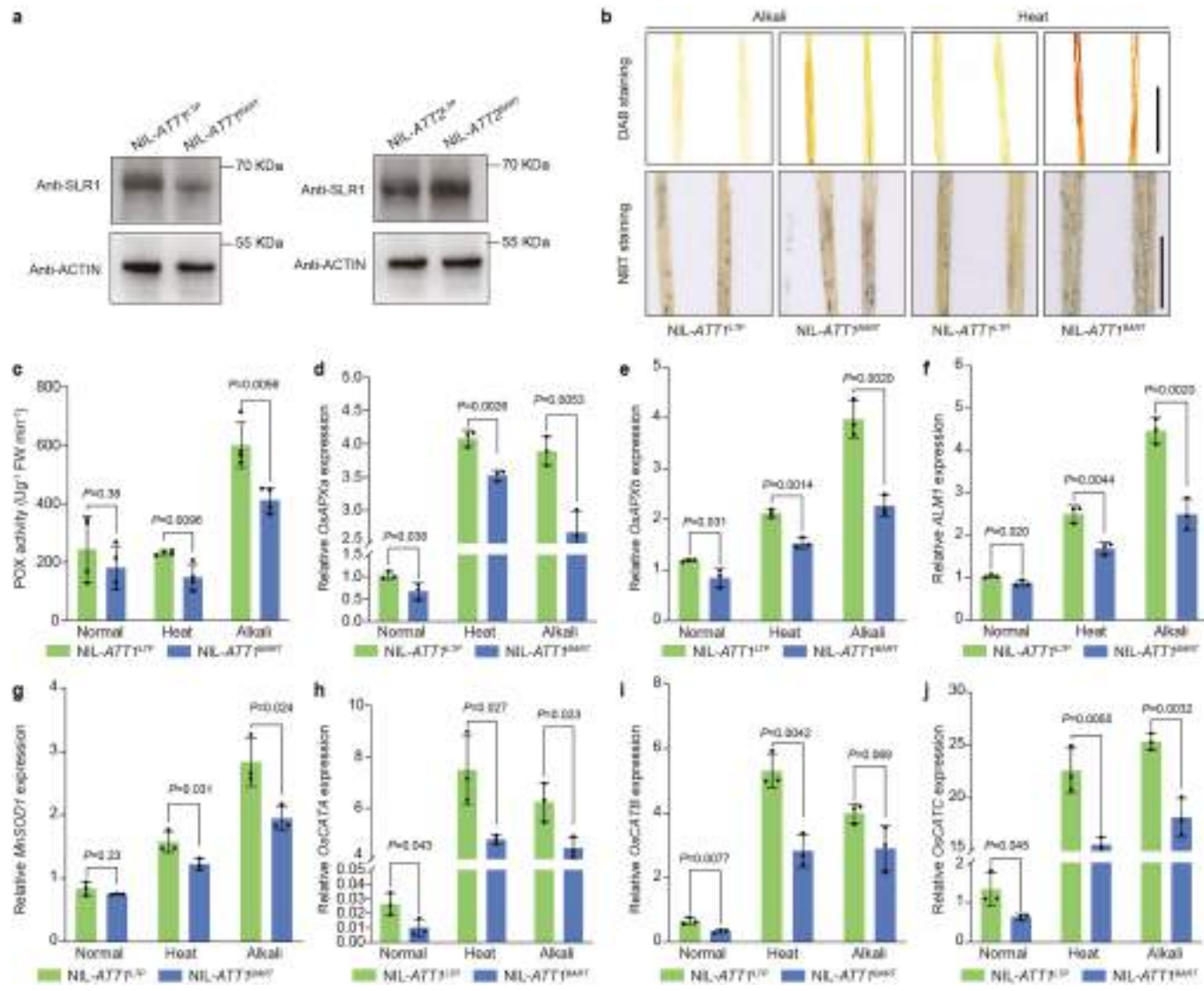
(45°C, RH > 90%, 1 d or 3 d). Scale bars, 1 cm. **f**, A proposed model showing that bioactive GAs accumulated highest in panicles compared to stems and leaves, and that the accumulation in stems, leaves and panicles was gradually repressed during alkali and heat-stressed conditions. **g,h**, Relative expression of *GA2ox* genes and *EUI* in LTP with or without alkali treatment (65 mM sodium bicarbonate, 24 h) and heat treatment (42°C, RH > 90%, 3 h). The values in **b-d,g,h** represent the mean \pm s.d.; $n = 3$, biologically independent samples; In **b-d**, the same lower-case letters indicate no significant difference at $p > 0.05$ as determined by two-way ANOVA with LSD test; In **g,h**, two-tailed Student's *t*-tests were used to determine *P* values.



Extended Data Fig. 4 | *ATT1* and *ATT2* modulate gibberellin synthesis regulating alkali-thermal tolerance. **a-c**, Phenotypes (**a**) and survival rates (**b,c**) of 12-day-old LTP seedlings in response to various concentrations of GA₃. **d-g**, Survival rates of NIL-*ATT1/2^{LTP}* (NIL-*ATT1^{LTP}*/*ATT2^{LTP}*), NIL-*ATT1^{BART}*, and NIL-*ATT2^{BART}* plants treated with 1 μM GA₃ (**d,e**) and 1 μM paclobutrazol (PAC) (**f,g**) under alkali (65 mM sodium bicarbonate, 14 days) (**d,f**) and heat (42 °C, RH > 90%, 28 h) (**e,g**) treatments on roots of 12-day-old rice seedlings. **h-j**, Phenotypes (**h**) and survival rates (**i-j**) of NIL-*ATT1/2^{LTP}* (NIL-*ATT1^{LTP}*/*ATT2^{LTP}*), NIL-*ATT1^{BART}*, and NIL-*ATT2^{BART}* plants treated with 1 μM GA₃ under alkali (65 mM sodium bicarbonate, 14 days) and heat (42 °C, RH > 90%, 28 h) treatments on

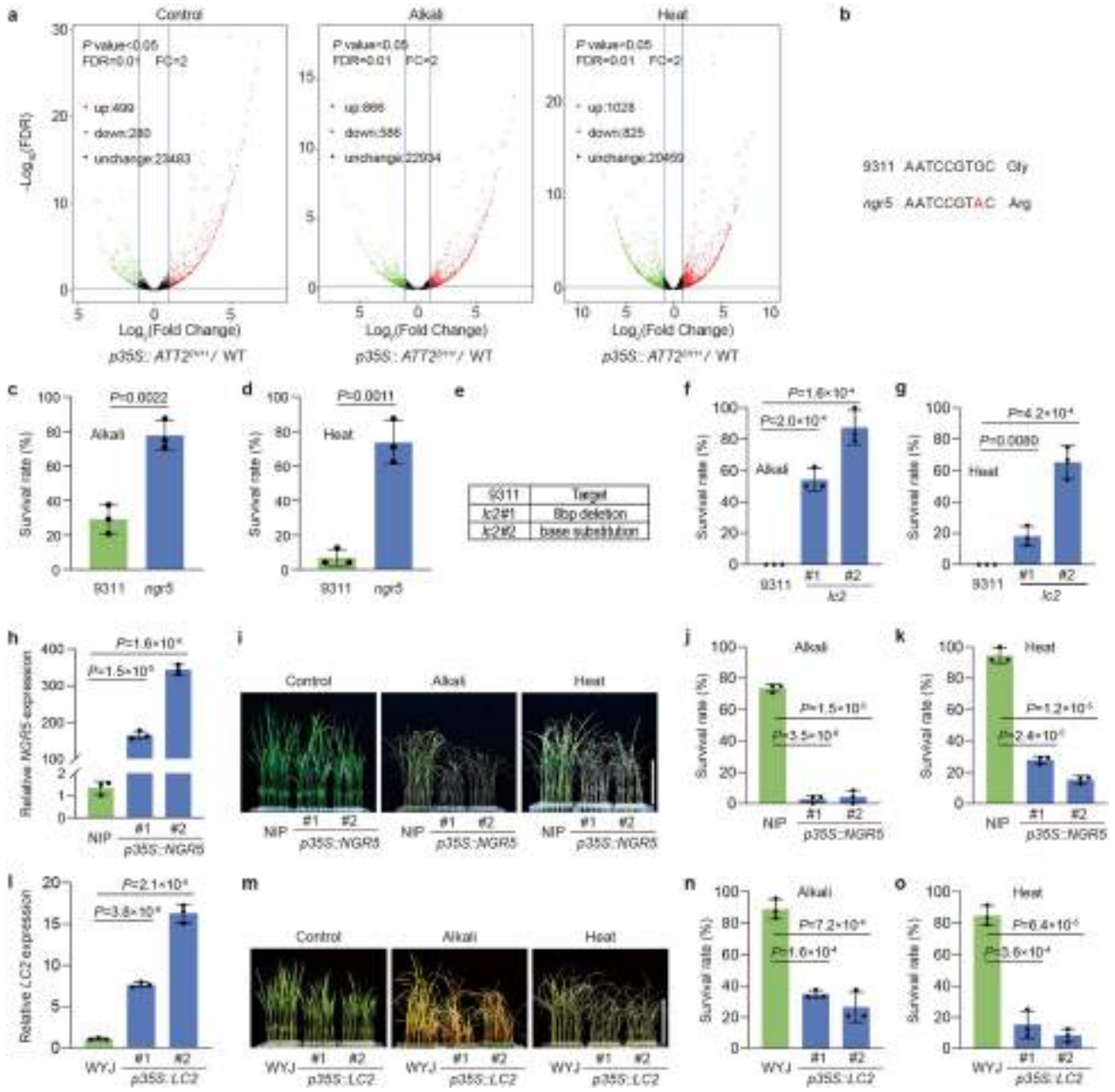
leaves of 12-day-old rice seedlings. Scale bars = 10 cm. **k-m**, Phenotypes (**k**) and survival rates (**l,m**) of NIL-*ATT1^{NP}* and NIL-*ATT1^{93II}* plants after alkali (65 mM sodium bicarbonate, 10 days) and heat (42 °C, RH > 90%, 20 h) treatments. Scale bars = 10 cm. **n**, Endogenous GA₁ and GA₄ contents in 12-day-old seedlings of NJ6 and *att1^{NP}*. The values in **b-g,i,j,l-n**, represent the mean ± s.d.; *n* = 3, biologically independent samples, each sample consisted of 24 seedlings; In **b-g,i,j,l-n**, the same lower-case letters indicate no significant difference at *p* > 0.05 as determined by two-way ANOVA with LSD test; In **l-n**, a two-tailed Student's *t*-tests was used to determine *P* values.

Article



Extended Data Fig. 5 | The relative expression of genes involved in ROS detoxification was higher in NIL-ATT1^{LTP} than in NIL-ATT1^{BART} under alkali-thermal treatment. **a**, Immunodetection of SLR1 in leaf tissues of NIL-ATT1^{LTP} and NIL-ATT1^{BART}, and NIL-ATT2^{LTP} and NIL-ATT2^{BART}. Actin was the loading control. The experiments were repeated independently three times with similar results. **b**, 3,3'-diaminobenzidine (DAB) and nitro-blue tetrazolium (NBT) staining were used to visualize H₂O₂ and O₂⁻, respectively, in alkali- and

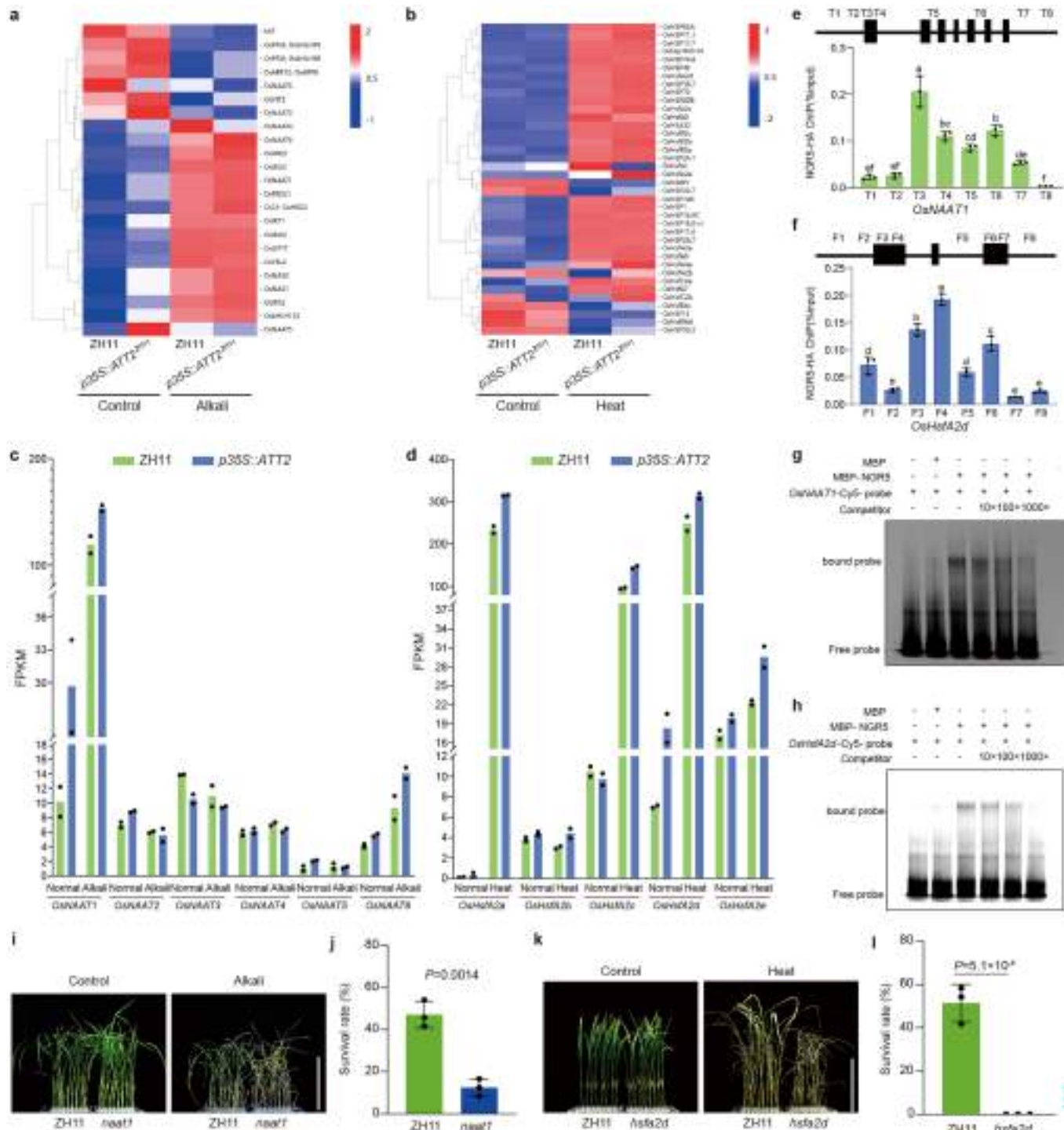
heat-treated rice leaves. Scale bars, 1 cm. **c-j**, Peroxidase (POX) activity (**c**) and the relative expression of genes (**d-j**) involved in ROS detoxification in NIL-ATT1^{LTP} and NIL-ATT1^{BART} under alkali (65 mM sodium bicarbonate, 24 h) and high temperature (42 °C, RH > 90%, 3 h) stress treatments. All experiments were conducted using 12-day-old seedlings. The values in **c-j** represent the mean ± s.d.; *n* = 3, biologically independent samples; two-tailed Student's *t*-tests were used to determine *P* values.



Extended Data Fig. 6 | NGR5 and LC2 are involved in alkali-thermal tolerance. **a**, Volcano plots showing the relative expression of genes associated with alkali (65 mM sodium bicarbonate, 24 h) and high temperature (42 °C, RH > 90%, 3 h) stress in ZH11 and overexpression-*ATT2^{ZH11}* line. The differentially expressed genes were analysed using the DESeq2 R package. Significant differentially expressed genes were determined using a standard procedure including adjusted *P* value (false discovery rate <0.05) and fold change ratio ($\log_2[FC] \geq 1$). $n = 2$ biologically independent samples. **b**, Nucleotide sequences of the target site in *NGR5* in the 9311 (WT) and the *ngr5* mutant showing the SNP (G-to-A transition) in the mutant allele leading to a predicted Gly to Arg substitution. **c,d**, Survival rates of 9311 and *ngr5* mutant plants under alkali treatment (**c**) (65 mM sodium bicarbonate, 12 days) and heat treatment (**d**) (42 °C, RH > 90%, 24 h). **e**, Mutation sites in *lc2* mutants. **f,g**, The survival rates of 9311 (WT) and

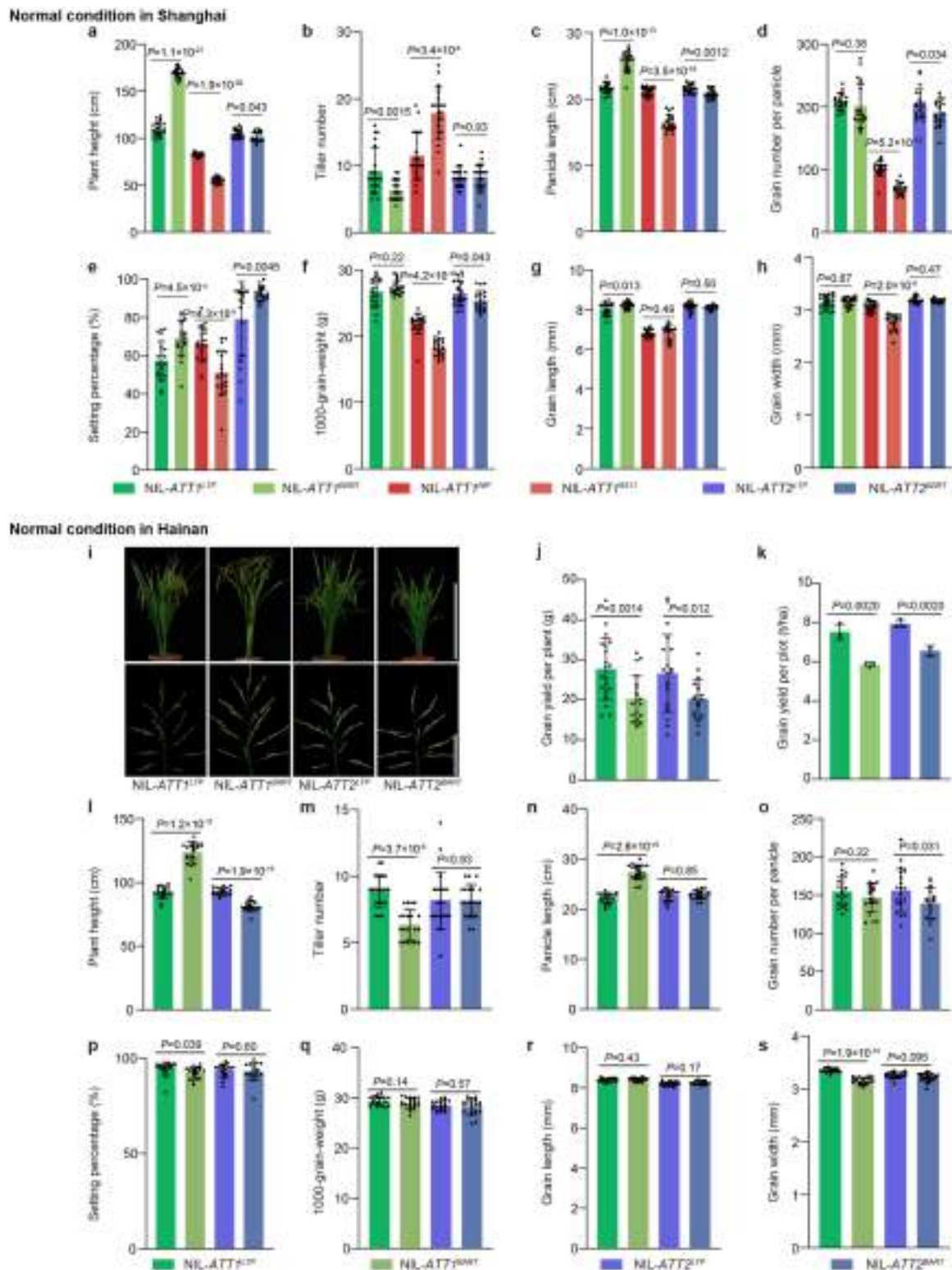
lc2 mutant plants under alkali treatment (**f**) (65 mM sodium bicarbonate, 12 days) and heat treatment (**g**) (42 °C, RH > 90%, 24 h). **h**, Expression of *NGR5* in ‘Nipponbare’ (NIP, WT) and *Pro3SS::NGR5* plants. **i-k**, Phenotypes (**i**) and survival rates (**j-k**) of ‘Nipponbare’ and *Pro3SS::NGR5* plants under alkali treatment (**j**) (65 mM sodium bicarbonate, 10 days), and heat treatment (**k**) (42 °C, RH > 90%, 20 h). **l**, Expression of *LC2* in ‘Wuyunjing’ (WYJ, WT) and *Pro3SS::LC2* overexpressing lines. **m-o**, Phenotypes (**m**) and survival rates (**n,o**) of ‘Wuyunjing’ and *Pro3SS::LC2* plants under normal conditions, alkali treatment (65 mM sodium bicarbonate, 10 days), and heat treatment (42 °C, RH > 90%, 20 h). Scale bars in (**i**) and (**m**) = 10 cm. The values in **c,d,f,g,h,j-l,n,o** represent the mean \pm s.d.; $n = 3$, biologically independent samples, each sample consisted of 24 seedlings; two-tailed Student’s *t*-tests were used to determine *P* values.

Article



Extended Data Fig. 7 | NGR5 regulates *OsNAAT1* and *OsHsfA2d* involve in alkali-thermal tolerance. **a,b**, Clustering heat maps showing the relative expression of genes associated with alkali (65 mM sodium bicarbonate, 24 h) (**a**) and high temperature (42 °C, RH > 90%, 3 h) (**b**) stress in ZH11 and overexpression-*ATT2*^{ZH11} line. **c,d**, Relative expression of rice genes associated with the alkali-thermal tolerance biological process in ZH11 and the *ATT2* overexpression line. FPKM, fragments per kilobase of transcript per million mapped reads. **a-d**, n = 2, biologically independent samples. **e,f**, ChIP-PCR experiments with *OsNAAT1* (**e**) and *OsHsfA2d* (**f**), n = 3, biologically independent samples. The black boxes indicate the exons, and T1-T8 and F1-F8 indicate the positions of randomly selected regions amplified by PCR. The graphs show the level of NGR5-HA-mediated enrichment (relative to input). **g,h**, Electrophoretic

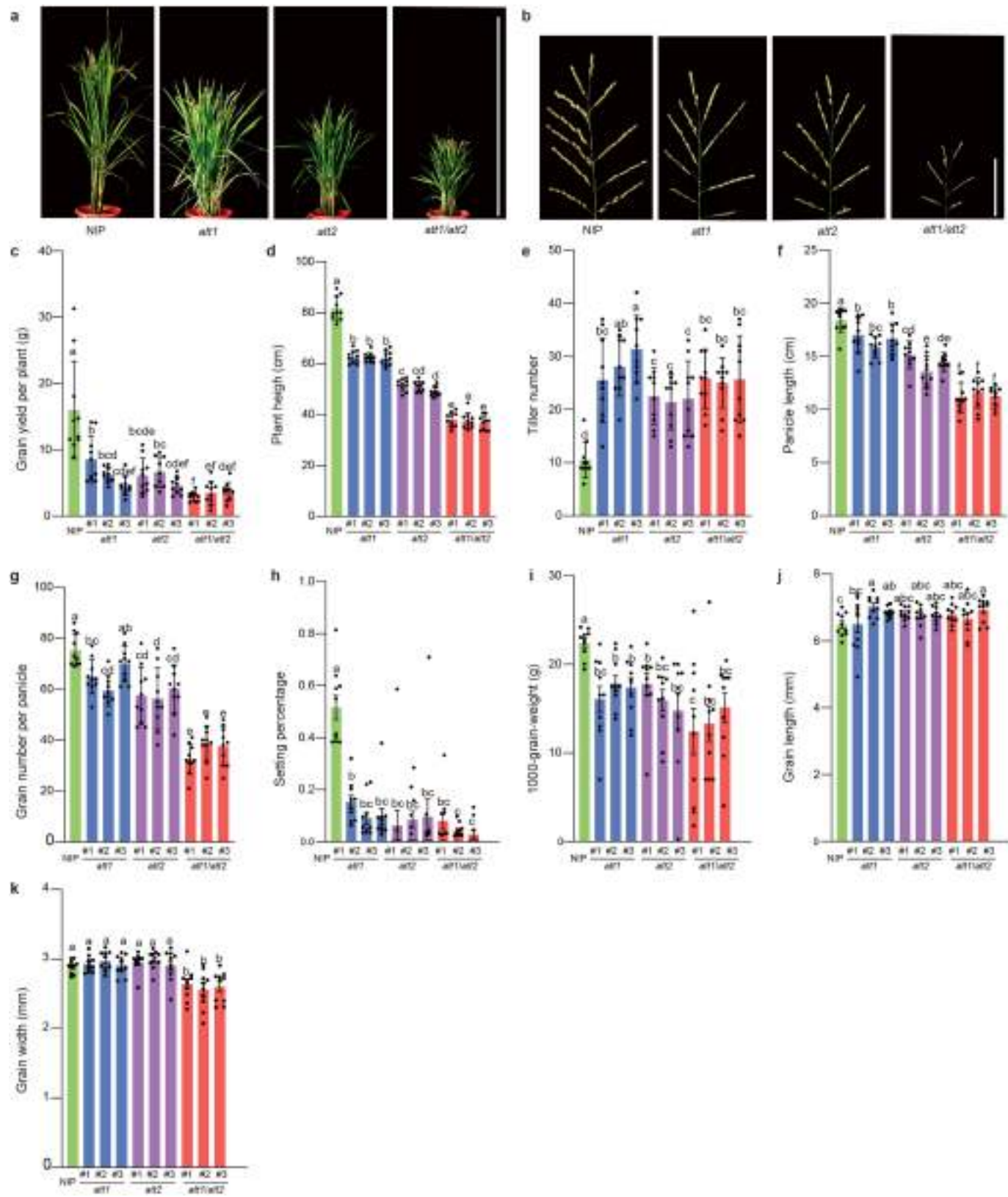
mobility shift assays (EMSA). DNA fragments T3 (**g**) and F4 (**h**) were incubated with MBP-NGR5 as indicated. Competition for NGR5 binding was performed with 10×, 100×, and 1,000× of the unlabeled probes. The experiments were repeated independently at least twice with similar results. **i-l**, Phenotypes (**i,k**) and survival rates (**j,l**) of the *naat1* and ZH11 (WT) plants subjected to alkali treatment (**i,j**) (65 mM sodium bicarbonate, 10 days) and *hsfa2d* and ZH11 plants subjected to heat treatment (**k,l**) (42 °C, RH > 90%, 20 h). In **i,k**, scale bars = 10 cm. The values in **e,f,g,h** represent the mean ± s.d.; In **j,l**, two-tailed Student's t-tests were used to determine P values; n = 3, biologically independent samples, each sample consisted of 24 plants; In **e,f**, the same lower-case letters indicate no significant difference at p > 0.05 as determined by two-way ANOVA with LSD test.



Extended Data Fig. 8 | Phenotypic characterization of NILs grown under normal conditions. **a-h**, Statistical analyses of plant height (a), tiller number (b), panicle length (c), grain number per panicle (d), seed setting percentage (e), 1,000-grain weight (f), grain length (g), and grain width (h) of NIL-*ATT1*^{LTP} and NIL-*ATT1*^{BART}, NIL-*ATT1*^{NIP} and NIL-*ATT1*^{93II}, and NIL-*ATT2*^{LTP} and NIL-*ATT2*^{BART} grown under normal field conditions in Shanghai. **i-s**, Plant architecture (upper panels; scale bars = 1 m) and panicle morphology (lower panels; scale bars = 10 cm) (i), and statistical

analysis of grain yield per plant (j) and grain yield per plot (k), plant height (l), tiller number (m), panicle length (n), grain number per panicle (o), seed setting percentage (p), 1,000-grain weight (q), grain length (r), and grain width (s) of NIL-*ATT1*^{LTP} and NIL-*ATT1*^{BART}, and NIL-*ATT2*^{LTP} and NIL-*ATT2*^{BART} grown under normal field conditions in Hainan. The values in **a-h,j-s** represent the mean \pm s.d.; In **a-h,j-l-s**, $n = 20$ plants; In **k**, $n = 3$ plots (each plot contained 180 plants); Two-tailed Student's *t*-tests were used to determine *P* values.

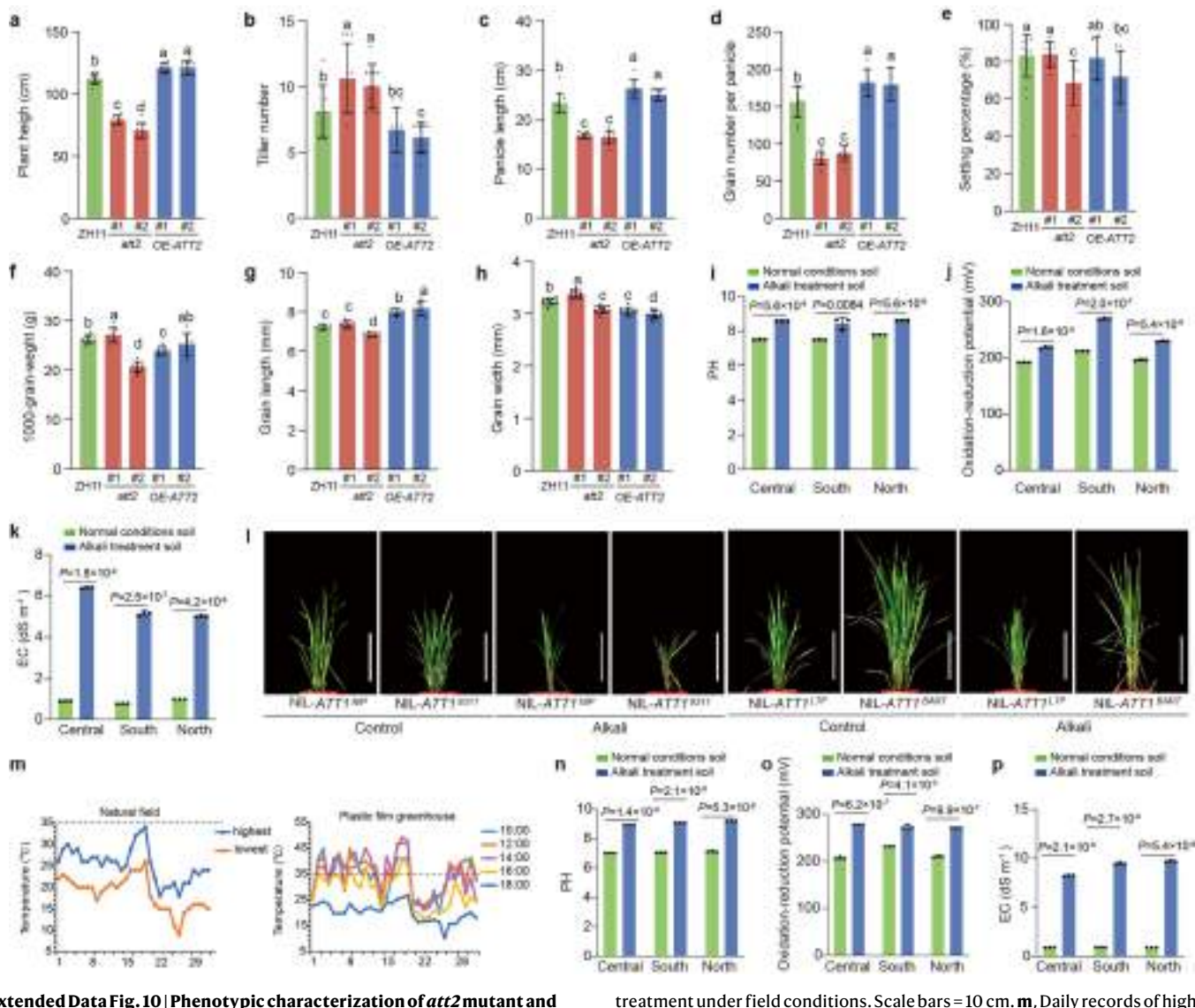
Article



Extended Data Fig. 9 | Phenotypic characterization of *att1*, *att2*, and *att1/att2* mutant plants in the 'Nipponbare' genetic background.

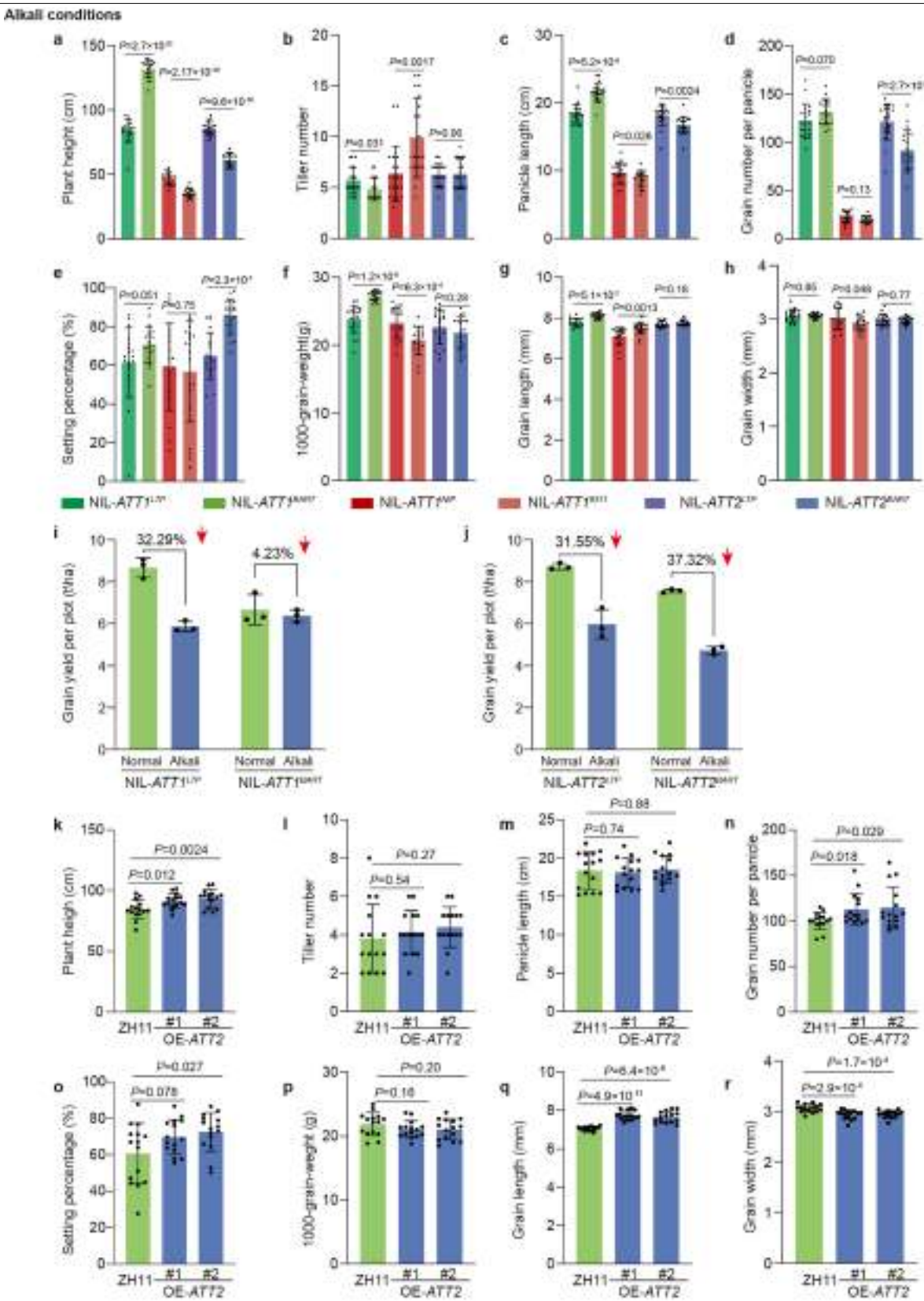
a, b. Comparison of the plant architecture at maturity (scale bar = 1 m) (a) and panicle morphology (scale bar = 10 cm) (b) in 'Nipponbare' (NIP, WT control), *att1*, *att2*, and *att1/att2* mutant plants. **c-k.** Statistical analysis of grain yield per plant (c), plant height (d), tiller number (e), panicle length (f), grain number per panicle (g), seed setting percentage (h), 1,000-grain weight (i), grain length (j), and grain width (k) of NIP control, *att1*, *att2*, and *att1/att2* mutant plants.

The values in c-k represent the mean \pm s.d. ($n = 10$ plants); The same letters indicate no significant difference at $p > 0.05$ as determined by two-way ANOVA with LSD test.



Extended Data Fig. 10 | Phenotypic characterization of *att2* mutant and *ATT2* overexpression transgenic plants grown normal conditions and physiological indices of alkali stress and temperature records in the field. **a-h**, Statistical analyses of plant height (**a**), tiller number (**b**), panicle length (**c**), grain number per panicle (**d**), seed setting percentage (**e**), 1,000-grain weight (**f**), grain length (**g**), and grain width (**h**) in ZH11 (WT), *att2* mutant, and overexpression-*ATT2* plants ($n=10$ plants). The values in **a-h** represent the mean \pm s.d. The same letters indicate no significant difference at $p > 0.05$ as determined by two-way ANOVA with LSD test. **i-k**, the pH, oxidation reduction potential, and electrical conductivity of normal and alkaline soils planted with NILs in summer 2022. **l**, Phenotypes of NIL-*ATT1*^{NIP} and NIL-*ATT1*^{Q3II}, and NIL-*ATT1*^{LTP} and NIL-*ATT1*^{BART} plants at the tillering stage with and without alkali treatment under field conditions. Scale bars = 10 cm. **m**, Daily records of high and low temperatures during the rice grain filling stages from early September to middle October 2022 from the weather station in Shanghai, China (left); Temperatures records collected with a GPRS-type temperature and humidity sensor (an instrument that can monitor temperature and humidity and store the data in real time) in a field greenhouse covered with plastic film (right). **n-p**, the pH, oxidation reduction potential, and electrical conductivity of normal and alkaline soils planted with ZH11 (WT) and overexpression-*ATT2* plants in summer 2023. The data in **i-k**, **n-p**, represent mean \pm s.d.; $n=3$, biologically independent samples; Two-tailed Student's *t*-tests were used to determine *P*values.

treatment under field conditions. Scale bars = 10 cm. **m**, Daily records of high and low temperatures during the rice grain filling stages from early September to middle October 2022 from the weather station in Shanghai, China (left); Temperatures records collected with a GPRS-type temperature and humidity sensor (an instrument that can monitor temperature and humidity and store the data in real time) in a field greenhouse covered with plastic film (right). **n-p**, the pH, oxidation reduction potential, and electrical conductivity of normal and alkaline soils planted with ZH11 (WT) and overexpression-*ATT2* plants in summer 2023. The data in **i-k**, **n-p**, represent mean \pm s.d.; $n=3$, biologically independent samples; Two-tailed Student's *t*-tests were used to determine *P*values.

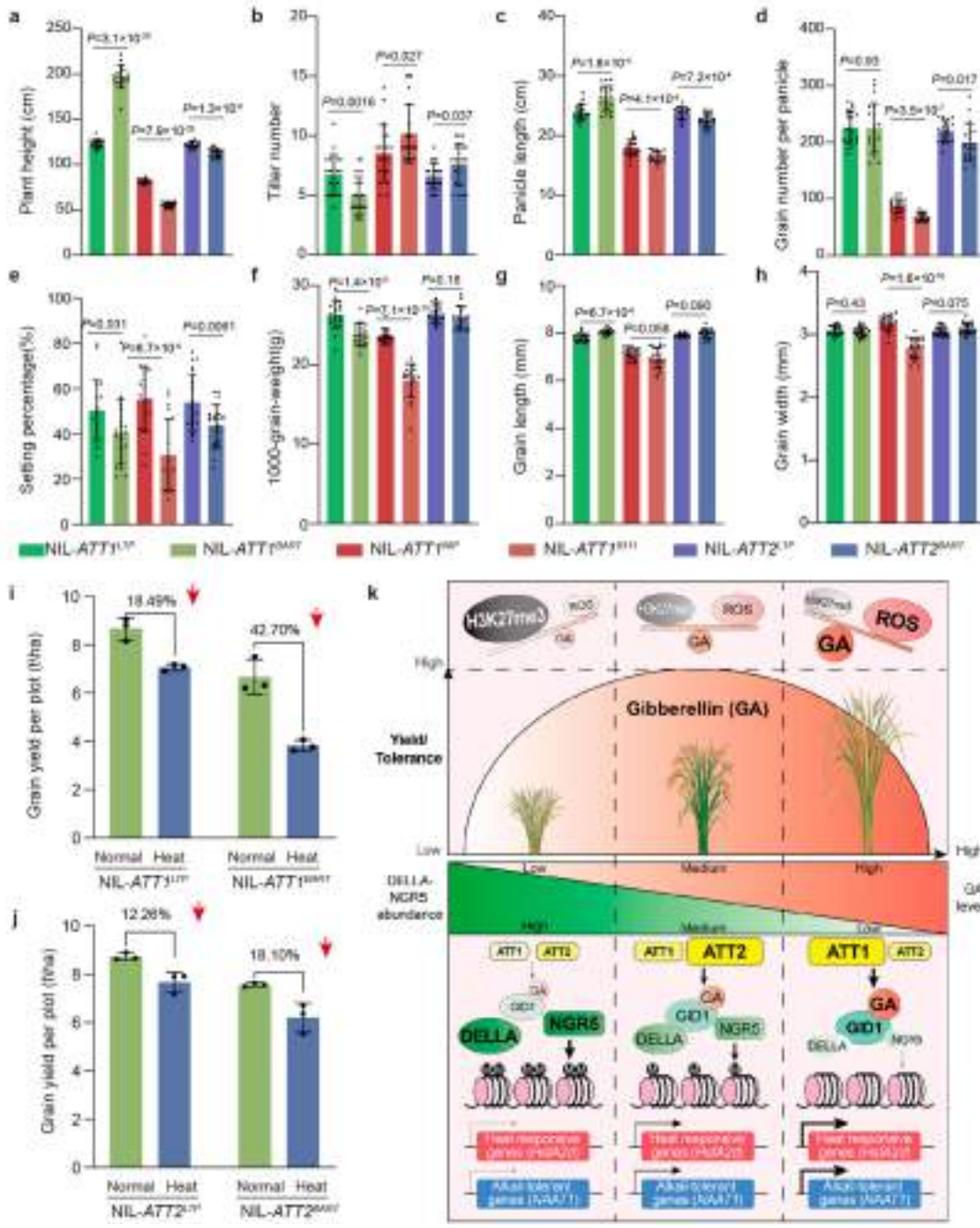


Extended Data Fig. 11 | Phenotypic characterization of NILs and ATT2 overexpression transgenic plants in the ZH11 genetic background under alkaline field conditions. **a-h.** Statistical analysis of plant height (a), tiller number (b), panicle length (c), grain number per panicle (d), setting percentage (e), 1,000-grain weight (f), grain length (g), and grain width (h) in NIL-ATT1^{LTP} and NIL-ATT1^{BART}, NIL-ATT1^{NIP} and NIL-ATT1^{93I}, and NIL-ATT2^{LTP} and NIL-ATT2^{BART} under alkaline field conditions in 2022 ($n = 20$ plants).

i,j. Statistical analysis of grain yield loss per plot in NIL-ATT1^{LTP} and NIL-ATT1^{BART} (i), and NIL-ATT2^{LTP} and NIL-ATT2^{BART} (j) under alkaline field conditions ($n = 3$ plots).

k-r. Statistical analyses of plant height (k), tiller number (l), panicle length (m), grain number per panicle (n), seed setting percentage (o), 1,000-grain weight (p), grain length (q), and grain width (r) in ZH11 (WT) and ATT2-overexpression plants under alkaline field conditions in 2023 ($n = 15$ plants). The values in a-h, k-r represent the mean \pm s.d.; Two-tailed Student's t-tests were used to determine P-values.

Heat conditions



Extended Data Fig. 12 | Phenotypic characterization of NILs under high temperature field conditions. **a-h**, Statistical analyses of plant height (**a**), tiller number (**b**), panicle length (**c**), grain number per panicle (**d**), seed setting percentage (**e**), 1,000-grain weight (**f**), grain length (**g**), and grain width (**h**) in NIL-ATT1^{LTP} and NIL-ATT1^{BART}, NIL-ATT1^{NP} and NIL-ATT1^{93I}, and NIL-ATT2^{LTP} and NIL-ATT2^{BART} under high temperature field conditions ($n = 20$ plants). The values in **a-j** represent the mean \pm s.d.; Two-tailed Student's *t*-tests were used to determine *P*values. **k**, A proposed model for the simultaneous improvement of grain yield and stress tolerance through precise regulation of GA levels. At low GA levels, DELLA accumulation and NGR5

stabilization leading to a genome-wide decrease in gene expression through H3K27me3 methylation, including genes for stress tolerance. At high GA levels, excessive accumulation of ROS produces deleterious effects on crops, especially in adverse environments, although stress-tolerance genes are highly expressed. Due to naturally occurring ATT1/SD1 variation, conventional GRVs contain low-medium levels of GA, resulting in semi-dwarf plant architecture and relatively high grain yields. Through enhanced ATT2 function or exogenous GA application, the level of GAs can be precisely fine-tuned to an optimal medium level to balance ROS concentrations and NGR5-mediated H3K27me3 levels, ultimately achieving further enhancement of both yield and alkali-thermal tolerance in Green Revolution rice varieties.

Reporting Summary

Nature Portfolio wishes to improve the reproducibility of the work that we publish. This form provides structure for consistency and transparency in reporting. For further information on Nature Portfolio policies, see our [Editorial Policies](#) and the [Editorial Policy Checklist](#).

Statistics

For all statistical analyses, confirm that the following items are present in the figure legend, table legend, main text, or Methods section.

n/a Confirmed

- The exact sample size (n) for each experimental group/condition, given as a discrete number and unit of measurement
- A statement on whether measurements were taken from distinct samples or whether the same sample was measured repeatedly
- The statistical test(s) used AND whether they are one- or two-sided
Only common tests should be described solely by name; describe more complex techniques in the Methods section.
- A description of all covariates tested
- A description of any assumptions or corrections, such as tests of normality and adjustment for multiple comparisons
- A full description of the statistical parameters including central tendency (e.g. means) or other basic estimates (e.g. regression coefficient) AND variation (e.g. standard deviation) or associated estimates of uncertainty (e.g. confidence intervals)
- For null hypothesis testing, the test statistic (e.g. F , t , r) with confidence intervals, effect sizes, degrees of freedom and P value noted
Give P values as exact values whenever suitable.
- For Bayesian analysis, information on the choice of priors and Markov chain Monte Carlo settings
- For hierarchical and complex designs, identification of the appropriate level for tests and full reporting of outcomes
- Estimates of effect sizes (e.g. Cohen's d , Pearson's r), indicating how they were calculated

Our web collection on [statistics for biologists](#) contains articles on many of the points above.

Software and code

Policy information about [availability of computer code](#)

Data collection	For heat treatment, chamber (Climacell EVO 707) was used. For qRT-qPCR and ChIP-qPCR data collection, QIAquant 96 2plex Real-Time PCR Systems was used. The DNA sequences were compared by MegAlign Pro (DNASTAR 11.0) detection. For POX activities and H2O2 contents, the AmplexTM Red Hydrogen (CAS:A22188) was used. Recombinant proteins were purified using the ÄKTA purification platform 25 (cytiva). Images from Immuno blotting were collected with the UVP Chemstudio touch (Analytik Jena AG).
Data analysis	Data were analyzed by microsoft EXCEL 2016 to perform two-tailed Student's t-test, differences between three or more groups were determined using two-way ANOVA with least significant difference (LSD) test. All analyses were performed using GraphPad Prism 8.0 software and the values are shown as mean \pm s.d. For RNA-seq data analysis, the differentially expressed genes were analysed using the DESeq2 package, DESeq2(v1.26.0). Significant differentially expressed genes were determined using a standard procedure including adjusted P value (false discovery rate < 0.05) and fold change ratio ($\log_2[FC] \geq 1$)

For manuscripts utilizing custom algorithms or software that are central to the research but not yet described in published literature, software must be made available to editors and reviewers. We strongly encourage code deposition in a community repository (e.g. GitHub). See the Nature Portfolio [guidelines for submitting code & software](#) for further information.

Data

Policy information about [availability of data](#)

All manuscripts must include a [data availability statement](#). This statement should provide the following information, where applicable:

- Accession codes, unique identifiers, or web links for publicly available datasets
- A description of any restrictions on data availability
- For clinical datasets or third party data, please ensure that the statement adheres to our [policy](#)

All data are available within this Article and its Supplementary Information. Original gel blots are shown in Supplementary Information Fig. 1. Original data points in graphs are shown in the Source Data files. The candidate genes in ATT1 and ATT2 chromosomal regions and accession number were obtained from the MSU database (<http://rice.plantbiology.msu.edu/>). The DNA next-generation genome sequencing data generated in this study have been deposited at the National Genomics Data Center under accession numbers (ID: CRA019914, <https://bigd.big.ac.cn/gsa/browse/CRA019914>). The RNA-seq data generated in this study have been deposited at the National Genomics Data Center under accession numbers (ID: CRA019913, <https://bigd.big.ac.cn/gsa/browse/CRA019913>). Source data are provided with this paper.

Research involving human participants, their data, or biological material

Policy information about studies with [human participants or human data](#). See also policy information about [sex, gender \(identity/presentation\), and sexual orientation](#) and [race, ethnicity and racism](#).

Reporting on sex and gender

N/A

Reporting on race, ethnicity, or other socially relevant groupings

N/A

Population characteristics

N/A

Recruitment

N/A

Ethics oversight

N/A

Note that full information on the approval of the study protocol must also be provided in the manuscript.

Field-specific reporting

Please select the one below that is the best fit for your research. If you are not sure, read the appropriate sections before making your selection.

Life sciences

Behavioural & social sciences

Ecological, evolutionary & environmental sciences

For a reference copy of the document with all sections, see nature.com/documents/nr-reporting-summary-flat.pdf

Life sciences study design

All studies must disclose on these points even when the disclosure is negative.

Sample size

No statistical methods were used to predetermine the sample size. The sample size was determined on the basis of preliminary experiments and previously published results of similar experiments, including the following literatures:
Alkali tolerance analysis in seedlings and plants: (DOI: 10.1038/s41467-019-14027-y, DOI: 10.1126/science.ade8416); Heat tolerance analysis in seedlings and plants: (DOI: 10.1038/s41467-020-19320-9, DOI: 10.1126/science.abo5721). Agronomic traits: (DOI: 10.1126/science.abi8455, DOI: 10.1038/s41467-023-38726-9).

Data exclusions

No data were excluded.

Replication

All experiments were independently and successfully conducted for at least two or three times. And the number of biological replicates is indicated in the figure legends.

Randomization

Plants were randomly assigned to normal-conditions or alkali and heat treatment groups for phenotype evaluation and sampling for subsequent analysis.

Blinding

Blinding is not applicable in this study as the research materials are plants. No bias was introduced into this study due to the fact that all relevant materials were randomly collected and treated identically. All experiments were conducted without prior knowledge of the results.

Reporting for specific materials, systems and methods

We require information from authors about some types of materials, experimental systems and methods used in many studies. Here, indicate whether each material, system or method listed is relevant to your study. If you are not sure if a list item applies to your research, read the appropriate section before selecting a response.

Materials & experimental systems

n/a	Involved in the study
<input type="checkbox"/>	<input checked="" type="checkbox"/> Antibodies
<input checked="" type="checkbox"/>	<input type="checkbox"/> Eukaryotic cell lines
<input checked="" type="checkbox"/>	<input type="checkbox"/> Palaeontology and archaeology
<input checked="" type="checkbox"/>	<input type="checkbox"/> Animals and other organisms
<input checked="" type="checkbox"/>	<input type="checkbox"/> Clinical data
<input checked="" type="checkbox"/>	<input type="checkbox"/> Dual use research of concern
<input type="checkbox"/>	<input checked="" type="checkbox"/> Plants

Methods

n/a	Involved in the study
<input checked="" type="checkbox"/>	<input type="checkbox"/> ChIP-seq
<input checked="" type="checkbox"/>	<input type="checkbox"/> Flow cytometry
<input checked="" type="checkbox"/>	<input type="checkbox"/> MRI-based neuroimaging

Antibodies

Antibodies used

For western blotting experiment, primary antibodies: Anti-SLR1 antibody (Abmart, P46081R1, 1:2,000 dilution, Rabbit), anti-ACTIN antibody (Abmart, M20009, 1:2,000 dilution, mouse); secondary antibody: goat-Anti-Mouse IgG (H+L) (Proteintech, SA00001-1, 1:10,000 dilution, goat), antibodies goat-Anti-Rabbit IgG (H+L) (Proteintech, SA00001-2, 1:10,000 dilution, goat). For ChIP-qPCR experiments: anti-H3K27me3 antibody (ABclonal, A2363, Rabbit), the anti-H3 antibody (ABclonal, A2348, Rabbit), and the anti-HA antibody (Proteintech, 51064-2-AP, Rabbit) is used, with a dilution of 1:200.

Validation

All antibody used are commercial and validations are based on the datasheet from the manufacturer and can found the detail information in the following list:
 Anti-SLR1-antibody: <https://www.abmart.com.cn/page.aspx?node=%2077%20&id=%20232550>
 anti-ACTIN antibody: <https://www.ab-mart.com.cn/page.aspx?node=%2059%20&id=%20985>
 goat-Anti-Mouse IgG (H+L): <https://www.ptgcn.com/products/HRP-conjugated-Affinipure-Goat-Anti-Mouse-IgG-H-L-secondary-antibody.htm>
 goat-Anti-Rabbit IgG (H+L): <https://www.ptgcn.com/products/HRP-conjugated-Affinipure-Goat-Anti-Rabbit-IgG-H-L-secondary-antibody.htm>
 anti-H3K27me3 antibody: <https://abclonal.com.cn/catalog/A2363>
 anti-H3 antibody: <https://abclonal.com.cn/catalog/A2348>
 anti-HA antibody: <https://www.ptgcn.com/products/HA-tag-Antibody-51064-2-AP.htm#product-information>

Dual use research of concern

Policy information about [dual use research of concern](#)

Hazards

Could the accidental, deliberate or reckless misuse of agents or technologies generated in the work, or the application of information presented in the manuscript, pose a threat to:

No	<input checked="" type="checkbox"/> Yes
<input checked="" type="checkbox"/>	<input type="checkbox"/> Public health
<input checked="" type="checkbox"/>	<input type="checkbox"/> National security
<input checked="" type="checkbox"/>	<input type="checkbox"/> Crops and/or livestock
<input checked="" type="checkbox"/>	<input type="checkbox"/> Ecosystems
<input checked="" type="checkbox"/>	<input type="checkbox"/> Any other significant area

Experiments of concern

Does the work involve any of these experiments of concern:

- | | |
|----|------------------------------------------------------------------------------------------------------|
| No | <input checked="" type="checkbox"/> Yes |
| | <input type="checkbox"/> Demonstrate how to render a vaccine ineffective |
| | <input type="checkbox"/> Confer resistance to therapeutically useful antibiotics or antiviral agents |
| | <input type="checkbox"/> Enhance the virulence of a pathogen or render a nonpathogen virulent |
| | <input type="checkbox"/> Increase transmissibility of a pathogen |
| | <input type="checkbox"/> Alter the host range of a pathogen |
| | <input type="checkbox"/> Enable evasion of diagnostic/detection modalities |
| | <input type="checkbox"/> Enable the weaponization of a biological agent or toxin |
| | <input type="checkbox"/> Any other potentially harmful combination of experiments and agents |

Plants

Seed stocks

O. barthii, 'Longtepū', ZH11, 'Songxianggengdao', p35S::ATT2 collected from our laboratory. The mutants att1, att1/att2, ngr5, gid1, lc2 and the transgenic overexpression lines p35S::ATT1, NGR5-HA and LC2-HA provided by Dr. Xiangdong Fu and Dr. Dabing Zhang

Novel plant genotypes

Transgenic lines were generated using CRISPR/Cas9 gene-editing constructs followed by Agrobacterium tumefaciens-mediated transformation. To generate rice att2 mutant lines in ZH11 background, we used two sgRNAs that target conserved regions (target1: CCCGTCGCAGTTCATATGGC, target2: CCACTCGACACGGCTGGGCAC). To generate rice att1 mutant lines in NIL-ATT1BART background, we used four sgRNAs that target conserved regions (target1: GGTGTACCAGAAACTGCG, target2: GCACTACCCGGACTTCACCT, target3: GAGGCCATTCTGTGGCCGAA, target4: GATCGCCGAACGGAAACGAAA). To generate rice att2 mutant lines in NIL-ATT2LTP and NIL-Na+HCO3- backgrounds, as well as att1/att2 double mutants lines in ZH11 background, we used four sgRNAs that target conserved regions (target1: GGTGTACCAGAAACTGCG, target2: GCACTACCCGGACTTCACCT, targets3/4: GATCGCCGAACGGAAACGAAA). To determine the expression of transgenic plants, qPCR and hygromycin label detection were used.

Authentication